UNIVERSITY OF STAVANGER

Performance of Enzyme-Catalyzed Single-E and Dual-E Homeostatic Controllers

by

Huimin Zhou

Master Thesis in Biological Chemistry

submitted to the
Faculty of Science and Technology
Department of Biology, Chemistry and Environmental Engineering

June 2020

UNIVERSITY OF STAVANGER

Abstract

Faculty of Science and Technology
Department of Biology, Chemistry and Environmental Engineering

Master Thesis in Biological Chemistry

by Huimin Zhou

Mathematical modeling has become an important tool in order to investigate the behavior of biological systems. The concept of homeostasis is central to our understanding how cells and organisms maintain an internal stability despite environmental or internal perturbations/insults. In this thesis the behavior and performance of two classes of homeostatic controllers are investigated. These two classes differ by the number of controller molecules involved in the homeostatic response. Single-E controllers contain one controller species, while dual-E controllers (antithetic controllers) contain two. A novel aspect of this thesis is the role enzymes can play in the performance of these controllers. For this purpose two controller motifs (negative feedback structures, motifs 5 and 2) have been investigated in detail. Enzymatic considerations included steady state and rapid equilibrium systems of ping-pong and ternary complex mechanisms for dual-E controllers and one-substrate Michaelis-Menten kinetics for single-E controllers. For the steady state systems reaction velocities were derived by the King-Altman method, which showed practically identical results in comparison with numerical calculations. For the motif 5 negative feedback arrangement a dual-E controller has a much better ability to withstand perturbations than a single-E controller. The reason for this is the fact that in dual-E controllers robust homeostasis can be achieved independently of the reaction order involving the removal of the two controller species E_1 and E_2. The single-E controller, on the other hand, requires zero-order or near zero-order removal kinetics with respect to its controller molecule E. When considering the ping-pong or ternary complex enzymatic mechanisms the dual-E controllers showed no significant differences in their homeostatic behaviors. Finally, the occurrence of enzyme-catalyzed dual-E controllers in physiology is discussed.

Acknowledgements

I cannot express enough thanks to my supervisor, Prof. Peter Ruoff for the continuous support throughout my master thesis. His broad knowledge, kindness, carefulness, patience and conscientiousness impressed me. I am extremely grateful for what he has offered me. And I could not imagine having a better supervisor besides Peter.

Secondly, I would like to express my gratitude to my engineer, Xiangming Xu for his encouragement and guide.

Finally, I am grateful to my parents who understand and support me taking this opportunity to study at UiS.

Contents

List of Figures

Abbreviations

ATP	**A**denosine **T**ri**P**hosphate
ADP	**A**denosine **D**i**P**hosphate
NAD$^+$	**N**icotinamide **A**denine **D**inucleotide

Introduction

The concept of "homeostasis" is more and more realized important to the public nowadays, particularly in physiology. But what is homeostasis? Homeostasis is, a concept, it is all the steady states of our human body, and other living organisms as well. However, it is not only the result, or the situation for steady state, but also includes the procedures to such a balancing tendency [1] in the internal environment when external disturbances.

The term of homeostasis was introduced by Walter B. Cannon with the Greek-derived prefix "homeo"[2, 3]. "Homeo" means *similar* and *like* instead of "same", which the specific property toward "to keep steady states within narrow limits" [3–5]. To stay homeostatic, difference mechanisms were discovered. Particularly, integral control, within negative feedback loop (Fig.1.1), has the remarkable ability to remain functional even under an extreme perturbation [5–8], which called *robust* homeostasis.

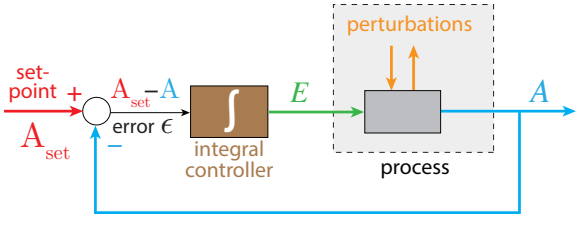

FIGURE 1.1: Scheme of the integral control within a negative feedback. A, the controlled variable, is corrected by using a negative feedback loop calculating the error(ϵ) as ϵ=A_{set}-A.

Basing on the negative feedback networks, a homestatic controller has one controlled variable A and one manipulated variable E, which E inhibites or activates acting on A' synthesis or degradation processes in order to stay homeostasis. With the development,

homestatic controllers are divided into two classes including four inflow controllers and four outflow controllers (Fig.1.2) [7]. As for inflow controllers, they compensate by adding A into the system while outflow controllers compensate by removing A from system.

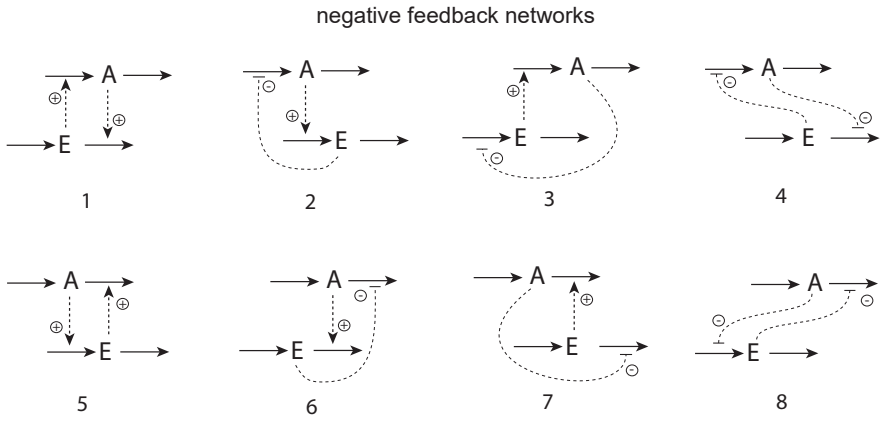

FIGURE 1.2: Scheme of the basic negative feedback networks including four inflow controllers (1-4) and four outflow controllers (5-8). The dashed lines refer to signal transduction originating from one species and affecting (stimulating or inhibiting) the other.

What's more, a new integral feedback mechanism, the so-called antithetic controller (Fig.1.3) [1, 9, 10], came out. Antithetic controller means a bimolecular replacement of single manipulated variable (E) by dual contoller pairs E_1 and E_2. The term "antithetic" is used, because of the opposing roles of the dual contoller pairs [11], which can consume each other to produce a product.

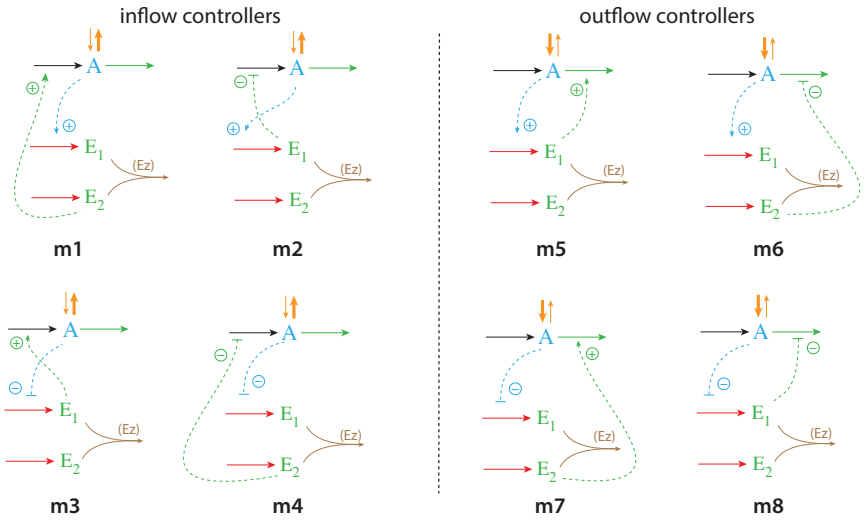

FIGURE 1.3: Scheme of the antithetic integral controller in combination with eight basic controller motifs. The removal of E_1 and E_2 can be either an uncatalyzed second-order degradation or a catalyzed one by an explicit enzyme (Ez).

In this thesis, an enzyme-catalyzed reaction is proposed which removes the manipulated variable species, E and E_1/E_2 (Fig.1.4) [12], called single-E and dual-E controller, respectively. This kind of enzymatic catalyzed removal of E and E_1/E_2 may be more realistic with respect to a living organism.

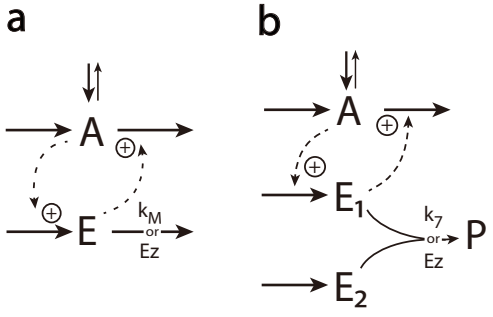

FIGURE 1.4: Scheme of integral antithetic controller based on motif 5. (**a**) Basic outflow controller, motif 5 with a single controll molecule E, under an uncatalyzed zero-order degradation or a catalyzed one by an enzyme (Ez). (**b**) Antithetic controller based on motif 5 under an uncatalyzed second-order removal of E_1 and E_2 or a catalyzed one by an enzyme (Ez).

Aim of thesis

The aim of this thesis is to introduce the new idea of enzyme-catalyzed antithetic controllers, i.e., where E_1 and E_2 are removed enzymatically. Especially, we compare the performance between catalyzed and uncatalyzed motif 5 and motif 2 controllers. More specifically, different mechanisms for the second-order reaction in the enzymatic antithetic controllers are taken into consideration including random order ternary complex mechanisms, compulsory order ternary complex mechanisms, and substitution (ping-pong) mechanisms (Fig.1.5) [13]. Reaction velocities determined by using the King-Altman steady state method are compared with numerical result and rapid equilibrium assumption.

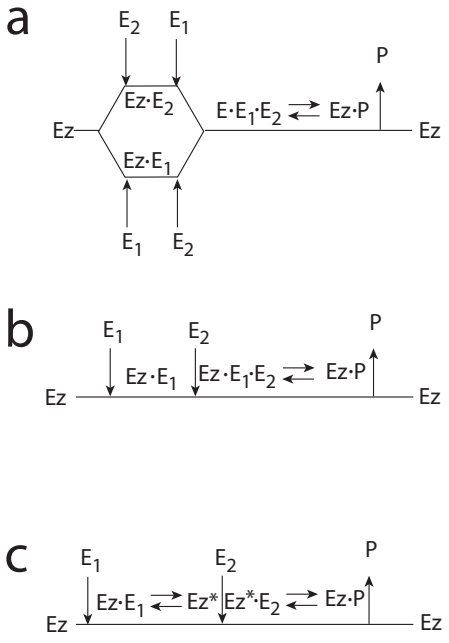

FIGURE 1.5: Scheme of two-substrate enzyme systems. (**a**) Random order ternary complex mechanism. (**b**) Compulsory order ternary complex mechanism. Note that here E_1 binds first then E_2 comes to bind with $E_1{\cdot}Ez$. The case that E_2 binds first is also taken into account in the thesis. (**c**) Substitution (ping-pong) mechanism. Note that here E_1 binds first then E_2 comes to bind with Ez^*. Also here the case that E_2 binds first to enzyme Ez is considered in the thesis.

This enzymatic depletion reaction may apply to all 8 kinds of motifs. In this thesis, I focus only on controller motifs 5 and 2 (Fig.1.3).

Materials and Methods

For mathematical modelling, computations were performed by using the Fortran subroutine LSODE [14], and in parallel, MATLAB (www.mathworks.com). Gnuplot (www.gnuplot.info) was used for plotting and Adobe Illustrator (www.adobe.com) was used for annotating pdfs. Concentrations of substances are represented by compound names without square brackets to make notation simpler. The "dot" notation is generally used for time derivatives. Concentrations and rate constants are given in arbitrary units (a.u.). Several runs for each individual model have been performed with different rate parameters. However, in this thesis, only the main results are presented.

Results and Discussion

Motif 5 uncatalyzed antithetic integral controller in comparison with zero-order

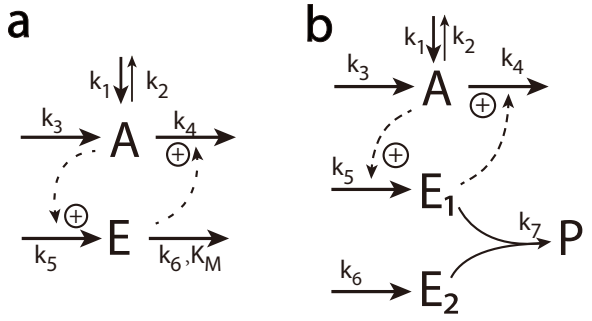

FIGURE 3.1: Scheme of integral antithetic controller based on motif 5. (**a**) Basic outflow controller, motif 5, uncatalyzed single-E controller. (**b**) Uncatalyzed antithetic dual-E controller based on motif 5.

Motif 5 (Fig.3.1 **a**) is an outflow controller compensating inflow perturbation by activating manipulated variable (E). Its set point (A_{set}) at steady state is defined by

$$\dot{A} = k_1 - k_2 \cdot A + k_3 - k_4 \cdot A \cdot E \tag{3.1}$$

$$\dot{E} = k_5 \cdot A - \frac{k_6 \cdot E}{K_M + E} \tag{3.2}$$

With assuming $\dot{E}$ equal to zero, then

$$A_{set} = \frac{k_6}{k_5} \cdot \frac{E}{K_M + E} \tag{3.3}$$

From Eq.3.3, when the value of K_M is particular small comparing with E, we can say that it is under zero-order condition. Thus, A_{set} becomes

$$A_{set} = \frac{k_6}{k_5} \tag{3.4}$$

The uncatalyzed antithetic dual-E controller from motif 5 (Fig.3.1**b**) includes two manipulated variables, E_1 and E_2, with the rate equations

$$\dot{A} = k_1 - k_2 \cdot A + k_3 - k_4 \cdot E_1 \cdot A \tag{3.5}$$

$$\dot{E_1} = k_5 \cdot A - k_7 \cdot E_1 \cdot E_2 \tag{3.6}$$

$$\dot{E_2} = k_6 - k_7 \cdot E_1 \cdot E_2 \tag{3.7}$$

For getting the steady state, the time derivations $\dot{E_1}$ and $\dot{E_2}$ are set to zero. Thus, the set point is given by combining Eq.3.6 and Eq.3.7.

$$\dot{E_1} - \dot{E_2} = k_5 \cdot A - k_6 = 0 \tag{3.8}$$

Therefore, for the above two controllers, the set point A_{set} is

$$A_{set} = \frac{k_6}{k_5} \tag{3.9}$$

The parameters k_1/k_2 represent inflow/outflow perturbation respectively (Fig.3.1). Since motif 5 is a outflow controller compensating for inflow perturbations, an increased perturbation (k_1) was applied to both controllers.

The results are showed in Fig.3.2. Both motif 5 uncatalyzed single-E controller and uncatalyzed antithetic dual-E controller have the ability to defend the their set points under the step-wise perturbation in Fig.3.2 (Row **a**). However, when k_1 is increased linearly in Fig.3.2 (Row **b**), both controllers show an off-set from the set point, which is increased with larger $\dot{k_1}$ and the off-set is same between controller motif 5 and uncatalyzed antithetic controller. Furthermore, in previous paper [5], the findings showed that controller motif 5 breaks down under a exponential/hyperbolic time-dependence perturbation and is not displayed here.

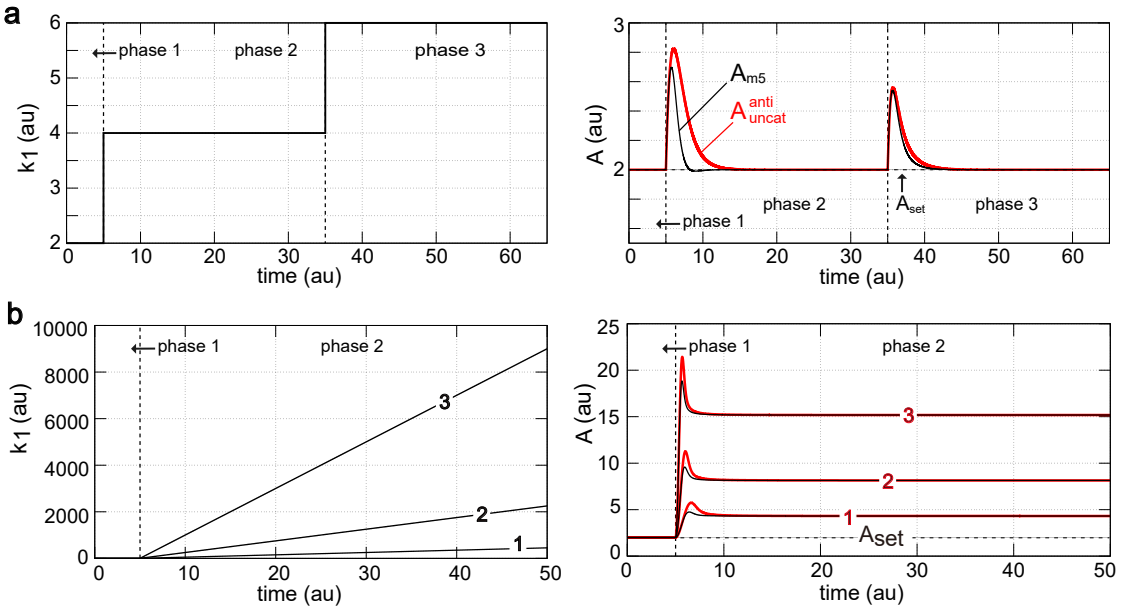

FIGURE 3.2: Comparison between uncatalyzed single-E motif 5 and corresponding antithetic dual-E controller (Fig.3.1). (Row **a**) Step-wise perturbation in k_1; left panel, phase 1 (0-5 time units): k_1=2, phase 2 (5-35 time units): k_1=4, phase 3 (35-65 time units): k_1=6; right panel, behavior of controlled variable A_{m5} for zero-order controller motif 5 in black and controlled variable A_{uncat}^{anti} for uncatalyzed antithetic controller in red. (Row **b**) Linear increases of k_1; left panel: phase 1 (0-5 time units): k_1 is kept constant at 2.0, phase 2 (5-50 time units): k_1 starts to increase with (1) $\dot{k_1}$=10.0, (2) $\dot{k_1}$=50.0, (3) $\dot{k_1}$=200.0; right panel: behavior of controlled variable A_{m5} for zero-order controller in black and controlled variable A_{uncat}^{anti} for uncatalyzed antithetic controller in red. Rate constants: k_2=1.0, k_3=1.0, k_4=1.0, k_5=1.0, k_6=2.0, k_7=2.0, K_M=1×10^{-6}.

Controller basing on motif 5: response times and accuracy

Response times and accuracy are two significant qualities for a homeostatic controller. Controller response time means the time when a perturbation enters the controller system until the system arrives at a steady state. Aggressiveness is a kind of property, which can influence the response times. In simple terms, different aggressiveness means the ratio of k_6/k_5=A_{set}, when A_{set} is kept constant but the values of k_6 and k_5 are changed. The term "accuracy" means how close the controller steady state to its theoretical set point.

In the following, the controller response times will be compared using two aspects, k_7 and aggressiveness, separately.

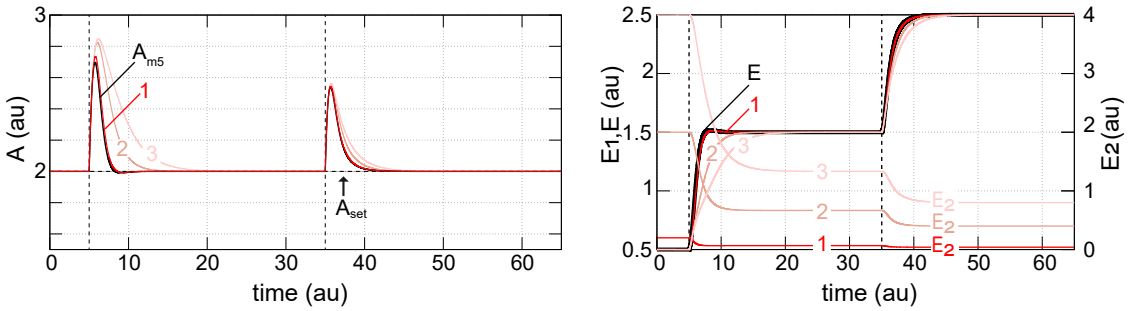

FIGURE 3.3: Comparing the response times with an increasing k_7 value in uncatalyzed antithetic controller. Left panel: behavior of controlled variables, A_{m5} for motif 5 in black and uncatalyzed antithetic controller outlined in red (1, 2, 3); Right panel: behavior of manipulated variables, E for motif 5 and E_1/E_2 for uncatalyzed antithetic controller. Perturbations k_1 and rate constants are the same as in Fig.3.2 row **a**, but with the following changes: 1, k_7=20.0; 2, k_7=2.0 (unaltered); 3, k_7=1.0.

Fig.3.3 shows that when applying an increased k_7 value, response times become shorter. Since k_7 is the parameter working on the degradations of E_1 and E_2, while a higher value of k_7, a rapid consumption of E_1 actives the compensatory outflow flux ($k_4 \cdot A \cdot E_1$) to oppose perturbation k_1. What's more, the response times of the uncatalyzed antithetic controller can be quick with an increased k_7. However,the uncatalyzed antithetic controller's response time will not be lower than the response time of motif 5, single-E controller.

As for aggressiveness, in this case, set point is kept at 2.0 all the time, while the value of k_5 and k_6 are altered.

It is obvious from Fig.3.4 that the response of both zero-order integral motif 5 and the uncatalyzed antithetic controller become faster with increasing aggressiveness and also approach minimum response times. The restriction that the antithetic (dual-E) controller will not be faster than the single-E controller appears to be caused by the following reason. When focusing on the behavior of manipulated variables (right panel of Fig.3.3 and right column of Fig.3.4), E_1 and E have a similar tendency to increase, while E_2 decreases. Thus, the level of E_1 cannot exceed E which is a kind of limitation to restrict the speed for how E_1 can change.

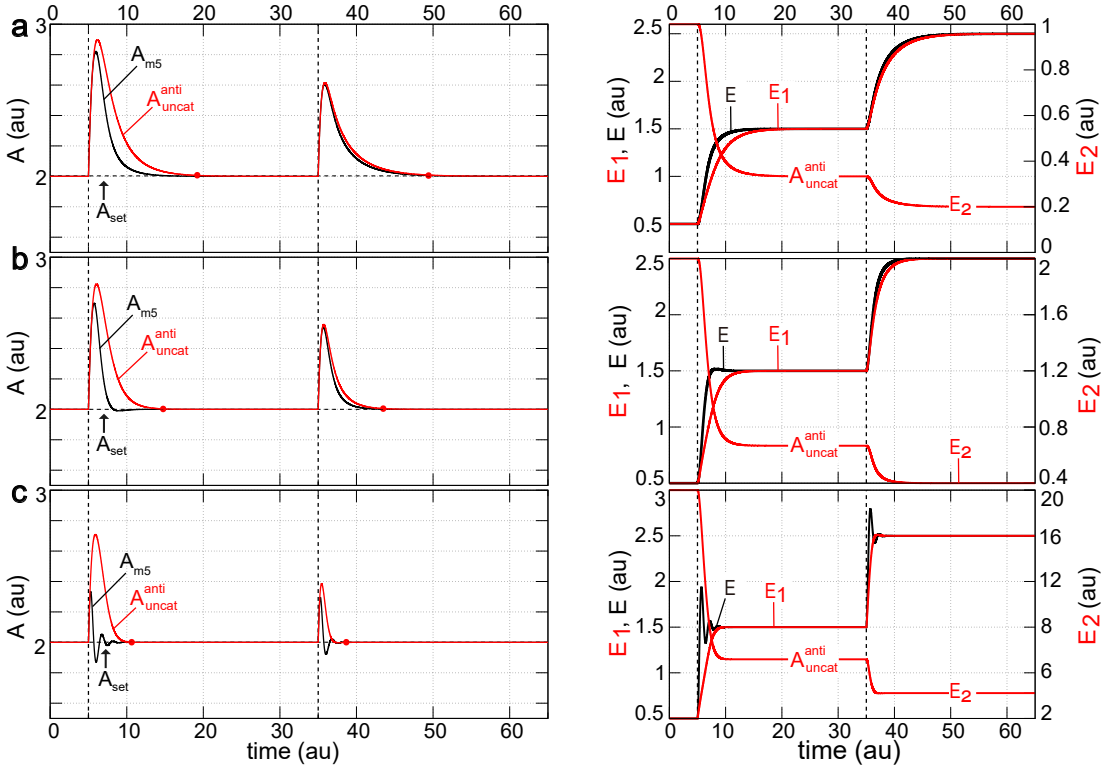

FIGURE 3.4: Comparing the response times with an increasing aggressiveness for zero-order motif 5 controller (in black) and uncatalyzed antithetic controller (in red). Perturbations k_1 and rate constants are the same as in Fig.3.2 row **a**, And keep the ratio(k_6/k_5) at 2.0, but with the following changes: Left column: row **a**, k_5=0.5, k_6=1.0; row **b**, k_5=1.0, k_6=2.0 (unaltered); row **c**, k_5=10.0, k_6=20.0. Right column: behavior of manipulated variables, E, E_1 and E_2. Note that red-dots indicate the time when controllers arrive at steady state.

In the following, the level of K_M is altered to find out how it influences controller accuracy. In this section, K_M plays a role only in motif 5 single-E controller, but not in the uncatalyzed antithetic controller.

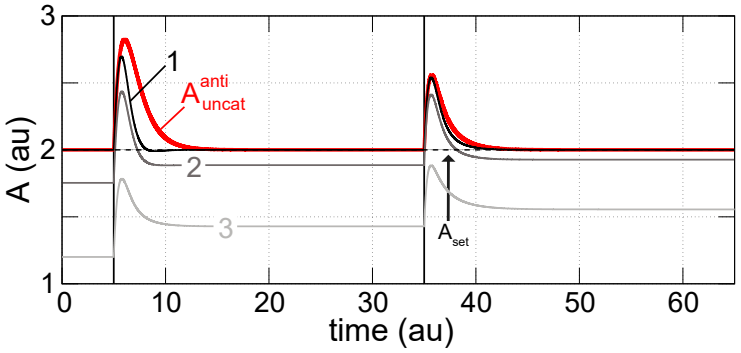

FIGURE 3.5: Comparison of accuracy with increasing K_M in zero-order (single-E) motif 5 controller. Perturbations k_1 and rate constants are the same as in Fig.3.2 row**a**, but with the following changes: 1, K_M=1×10^{-6} (unaltered); 2, K_M=1×10^{-1}; 3, K_M=1.0.

From Eq.3.3, we know that K_M plays an important role in calculating the theoretical set point of basic motif 5 when it works under zero-order condition (low K_M). For the result (Fig.3.5), an increased K_M would increase the off-set from its theoretical set point A_{set}. Interestingly, from phase 1 to 3 with increased perturbations, the off-set becomes smaller. This would be a typical phenomenon for motif 5 because it is an activation kinetic outflow controller, where a large inflow perturbation of A will increase E such that the term $E/(K_M + E)$ (Eq.3.3) becomes smaller and smaller.
And this increasing accuracy with increasing k_1 should adopt for all motif 5-based controllers including the uncatalyzed antithetic controller and the catalyzed antithetic controllers in the following section.
Therefore, in fact, both lower K_M and higher perturbation (k_1) can increase the accuracy. Response time can be reduced by either higher k_7 or higher aggressiveness.

Motif 5 antithetic controller with enzymatic catalyzed mechanisms

In the following, comparisons are shown between controller motif 5 and the antithetic controller with an explicitly enzyme-catalyzed degradation of the manipulated variables, E and E_1/E_2.

Mechanism of motif 5 catalyzed single-E and dual-E controllers and the rate equations derivation

Before comparison, all the interested controllers are introduced in detail including the mechanism in schemes, rate equations derivation, and the velocity calculated by using rapid equilibrium assumption and King-Altman steady state mechanism.

Motif 5 single-E controller with Michaelis-Menten degradation of E

The scheme of motif 5 single-E controller is in Fig.3.6 below.

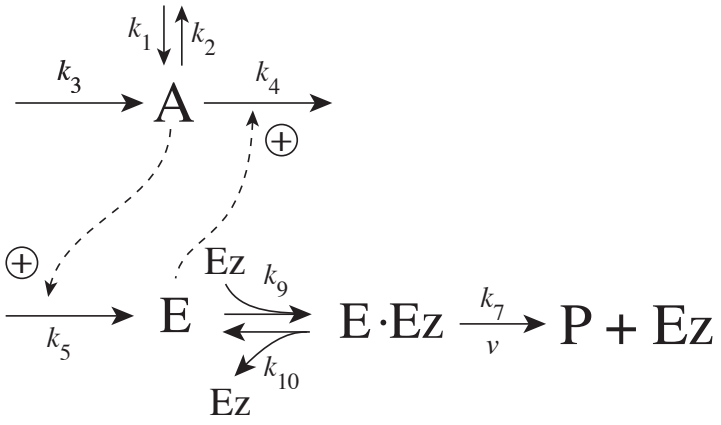

FIGURE 3.6: Motif 5 single-E controller: removal of E by enzyme Ez using a Michaelis-Menten mechanism.

The rate equations for motif 5 single-E controller are as follows:

$$\dot{A} = k_1 - k_2 \cdot A + k_3 - k_4 \cdot E \cdot A \tag{3.10}$$

$$\dot{E} = k_5 \cdot A - k_9 \cdot (E) \cdot (Ez) + k_{10} \cdot (E \cdot Ez) \tag{3.11}$$

$$\dot{Ez} = -k_9 \cdot (Ez) \cdot (E) + k_{10} \cdot (E \cdot Ez) + k_7 \cdot (E \cdot Ez) \tag{3.12}$$

$$\frac{d(E \cdot Ez)}{dt} = k_9 \cdot (Ez) \cdot (E) - k_{10} \cdot (E \cdot Ez) - k_7 \cdot (E \cdot Ez) \tag{3.13}$$

In order to find the set point, Eq.3.11 and Eq.3.12 are set to zero at steady state. Then

$$A \cdot k_5 = k_9 \cdot (E) \cdot (Ez) - k_{10} \cdot (E \cdot Ez) \tag{3.14}$$

$$k_7 \cdot (E \cdot Ez) = k_9 \cdot (Ez) \cdot (E) - k_{10} \cdot (E \cdot Ez) \tag{3.15}$$

$$A \cdot k_5 = k_7 \cdot (E \cdot Ez) \tag{3.16}$$

And Eq.3.16 combines with the conversion from Eq.3.13. When it is under zero-order condition, the set point A_{set}, is

$$A_{set} = \frac{k_7 \cdot Ez_{tot}}{k_5} \tag{3.17}$$

Here, Ez_{tot} means the total enzyme concentration, i.e.,

$$Ez_{tot} = (Ez) + (E \cdot Ez) \tag{3.18}$$

Motif 5 dual-E controller with random order ternary complex mechanism

Fig.3.7 is the scheme of the motif 5 dual-E controller with random order ternary complex mechanism.

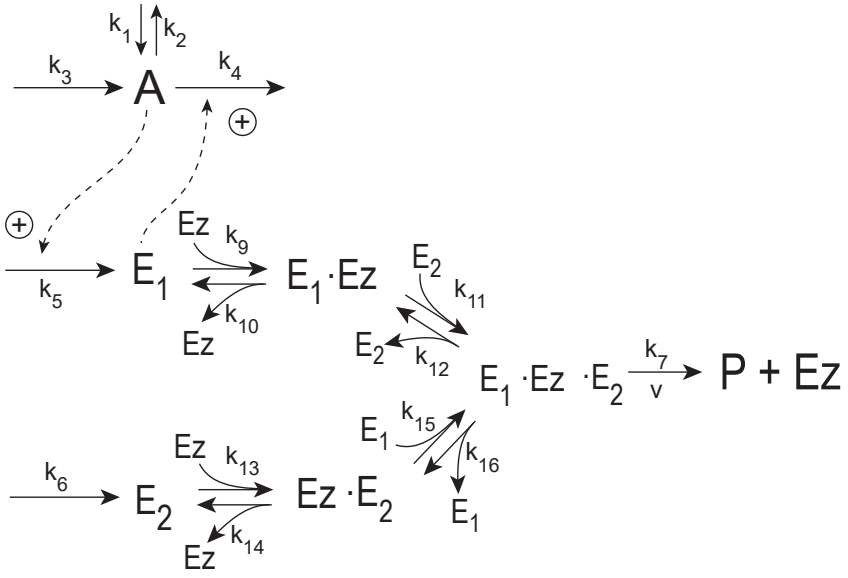

FIGURE 3.7: Motif 5 dual-E controller: removal of E_1 and E_2 by enzyme Ez using a ternary complex mechanism with random binding order.

The rate equations are,

$$\dot{A} = k_1 - k_2 \cdot A + k_3 - k_4 \cdot E_1 \cdot A \tag{3.19}$$

$$\dot{E_1} = k_5 \cdot A - k_9 \cdot (E_1) \cdot (E_2) + k_{10} \cdot (E_1 \cdot Ez) - k_{15} \cdot (E_1) \cdot (Ez \cdot E_2) + k_{16} \cdot (E_1 \cdot Ez \cdot E_2) \tag{3.20}$$

$$\dot{E_2} = k_6 - k_{13} \cdot E_2 \cdot Ez + k_{14} (Ez \cdot E_2) - k_{11} \cdot (E_1 \cdot Ez) \cdot E_2 + k_{12} \cdot (E_1 \cdot Ez \cdot E_2) \tag{3.21}$$

$$\dot{Ez} = -k_9 \cdot (E_1) \cdot (Ez) + k_{10} \cdot (E_1 \cdot Ez) + k_7 \cdot (E_1 \cdot Ez \cdot E_2) - k_{13} \cdot (Ez) \cdot (E_2) + k_{14} \cdot (Ez \cdot E_2) \tag{3.22}$$

$$\frac{d(E_1 \cdot Ez)}{dt} = k_9 \cdot (E_1) \cdot (E_2) - k_{10} \cdot (E_1 \cdot Ez) - k_{11} \cdot (E_1 \cdot Ez) \cdot (E_2) + k_{12} \cdot (E_1 \cdot Ez \cdot E_2) \tag{3.23}$$

$$\frac{d(E_1 \cdot Ez \cdot E_2)}{dt} = k_{11} \cdot (E_1 \cdot Ez) \cdot (E_2) - k_{12} \cdot (E_1 \cdot Ez \cdot E_2) - k_7 \cdot (E_1 \cdot Ez \cdot E_2) + k_{15} \cdot (Ez \cdot E_2) \cdot (E_1) - k_{16} \cdot (E_1 \cdot Ez \cdot E_2) \tag{3.24}$$

$$\frac{d(Ez \cdot E_2)}{dt} = k_{13} \cdot (E_2) \cdot (Ez) - k_{14} \cdot (Ez \cdot E_2) - k_{15} (Ez \cdot E_2) \cdot (E_1) + k_{16} \cdot (E_1 \cdot Ez \cdot E_2) \tag{3.25}$$

The reaction velocity v is,

$$v = \dot{P} = k_7 \cdot (E_1 \cdot Ez \cdot E_2) \tag{3.26}$$

With a rapid equilibrium assumption, we have the equilibrium expressions as follows:

$$K_{M1} = \frac{(Ez) \cdot (E_1)}{(E_1 \cdot Ez)} = \frac{k_{10}}{k_9} \tag{3.27}$$

$$K_{M2} = \frac{(E_1 \cdot Ez) \cdot (E_2)}{(E_1 \cdot Ez \cdot E_2)} = \frac{k_{12}}{k_{11}} \tag{3.28}$$

$$K_{M3} = \frac{(Ez) \cdot (E_2)}{(Ez \cdot E_2)} = \frac{k_{14}}{k_{13}} \tag{3.29}$$

$$K_{M4} = \frac{(E_1) \cdot (Ez \cdot E_2)}{(E_1 \cdot Ez \cdot E_2)} = \frac{k_{16}}{k_{15}} \tag{3.30}$$

In order to get the expression of v in Eq.3.26, the total concentration of Ez is Ez_{tot},

$$Ez_{tot} = (E_1 \cdot Ez) + (Ez \cdot E_2) + (E_1 \cdot Ez \cdot E_2) + (Ez) \tag{3.31}$$

and

$$(E_1 \cdot Ez) = \frac{K_{M2}}{(E_2)} \cdot (E_1 \cdot Ez \cdot E_2) \tag{3.32}$$

$$(Ez \cdot E_2) = \frac{K_{M4}}{(E_1)} \cdot (E_1 \cdot Ez \cdot E_2) \tag{3.33}$$

$$(Ez) = \frac{K_{M1}}{(E_1)} \cdot (E_1 \cdot Ez) = \frac{K_{M1}}{(E_1)} \cdot \frac{K_{M2}}{(E_2)} \cdot (E_1 \cdot Ez \cdot E_2) \tag{3.34}$$

Thus,

$$Ez_{tot} = (\frac{K_{M2}}{(E_2)} + \frac{K_{M4}}{(E_1)} + \frac{K_{M1} \cdot K_{M2}}{(E_1) \cdot (E_2)} + 1) \cdot (E_1 \cdot Ez \cdot E_2) \tag{3.35}$$

The rapid equilibrium approximation for velocity, v, is then

$$v^{random}_{rapid\_eq} = \frac{k_7 \cdot Ez_{tot}}{(1 + \frac{K_{M4}}{(E_1)} + \frac{K_{M2}}{(E_2)} + \frac{K_{M1} \cdot K_{M2}}{(E_1) \cdot (E_2)})} = \frac{V_{max}}{(1 + \frac{K_{M4}}{(E_1)} + \frac{K_{M2}}{(E_2)} + \frac{K_{M1} \cdot K_{M2}}{(E_1) \cdot (E_2)})} \tag{3.36}$$

Note that K_{M1}, K_{M2}, K_{M3} and K_{M4} should comply with the principle called *detailed balance* [15], i.e.,

$$K_{M1} \cdot K_{M2} = K_{M3} \cdot K_{M4} \tag{3.37}$$

However, the expression of v becomes much complex with a steady state assumption and it comes up later with the King-Altman method.

Actually, the set point of the dual-E controller is dependent on the concentration of E_2,

which can be divided into two cases. When the concentration value of E_2 is much lower than E_1, the set point would be same as for the uncatalyzed one (3.9),

$$A_{set} = \frac{k_6}{k_5} \tag{3.38}$$

But, when E_2 is relative large, the dual-E controller gets the same set point (3.17) as the single-E controller,

$$A_{set} = \frac{k_7 \cdot Ez_{tot}}{k_5} \tag{3.39}$$

In this thesis, the King-Altman method is also taken into consideration to compare the numerical velocity with the velocity using a steady state approach. Fig.3.8 is the scheme of the motif 5 random order dual-E controller using the King-Altman method.

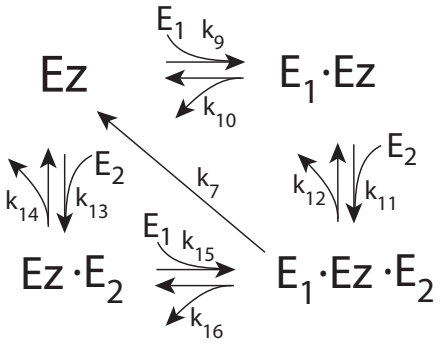

FIGURE 3.8: The scheme of motif 5 dual-E controller with random order ternary complex mechanism using the King-Altman method. The four enzymatic species are arranged in form of a square.

For the free enzyme Ez, its formation is indicated by the arrow in the fractional numerator below (3.40).

$$\frac{Ez}{Ez_{tot}} = \frac{\uparrow\uparrow + \uparrow\rightarrow + \uparrow\downarrow + \uparrow\leftarrow + \uparrow\nwarrow + \searrow\downarrow + \searrow\rightarrow + \uparrow\nwarrow\downarrow}{D} \tag{3.40}$$

Then, apply the coefficient to its represented arrow:

$$\begin{aligned} \frac{\mathrm{Ez}}{\mathrm{Ez_{tot}}} = & \frac{k_{14} \cdot k_{10} \cdot k_{12} + k_{15} \cdot E_1 \cdot k_{12} \cdot k_{10} + k_{11} \cdot E_2 \cdot k_{16} \cdot k_{14}}{D} \\ & \frac{+k_{16} \cdot k_{14} \cdot k_{10} + k_7 \cdot k_{14} \cdot k_{10} + k_{11} \cdot E_2 \cdot k_{15} \cdot E_1 \cdot k_7}{D} \\ & \frac{+k_{10} \cdot k_{15} \cdot E_1 \cdot k_7 + k_{14} \cdot k_{11} \cdot E_2 \cdot k_7}{D} \end{aligned} \tag{3.41}$$

For enzymatic species $E_1{\cdot}Ez$, we get the ratio

$$\frac{(\mathrm{E_1{\cdot}Ez})}{\mathrm{Ez_{tot}}} = \frac{\quad + \quad + \quad + \quad + \quad + \quad + \quad}{D}$$
$$= \frac{k_{14}{\cdot}k_9{\cdot}E_1{\cdot}k_{12} + k_9{\cdot}E_1{\cdot}k_{12}{\cdot}k_{15}{\cdot}E_1 + k_{13}{\cdot}E_2{\cdot}k_{15}{\cdot}E_1{\cdot}k_{12}}{D}$$
$$\frac{+k_{16}{\cdot}k_{14}{\cdot}k_9{\cdot}E_1 + k_{14}{\cdot}k_7{\cdot}k_9{\cdot}E_1 + k_{15}{\cdot}E_1{\cdot}k_7{\cdot}k_9{\cdot}E_1}{D} \tag{3.42}$$

For enzymatic species $E_1{\cdot}Ez{\cdot}E_2$, we get the ratio

$$\frac{(\mathrm{E_1{\cdot}Ez{\cdot}E_2})}{\mathrm{Ez_{tot}}} = \frac{\quad + \quad + \quad + \quad + \quad + \quad + \quad}{D}$$
$$= \frac{k_{14}{\cdot}k_9{\cdot}E_1{\cdot}k_{11}{\cdot}E_2 + k_9{\cdot}E_1{\cdot}k_{11}{\cdot}E_2{\cdot}k_{15}{\cdot}E_1 + k_{13}{\cdot}E_2{\cdot}k_{15}{\cdot}E_1{\cdot}k_{11}{\cdot}E_2}{D}$$
$$\frac{+k_{10}{\cdot}k_{13}{\cdot}E_2{\cdot}k_{15}{\cdot}E_1}{D} \tag{3.43}$$

For enzymatic species $Ez{\cdot}E_2$, we get the ratio

$$\frac{(\mathrm{Ez{\cdot}E_2})}{\mathrm{Ez_{tot}}} = \frac{\quad + \quad + \quad + \quad + \quad + \quad + \quad}{D}$$
$$= \frac{k_{13}{\cdot}E_2{\cdot}k_{10}{\cdot}k_{12} + k_{16}{\cdot}k_{13}{\cdot}E_2{\cdot}k_{10} + k_{13}{\cdot}E_2{\cdot}k_{16}{\cdot}k_{11}{\cdot}E_1}{D}$$
$$\frac{+k_{10}{\cdot}k_{13}{\cdot}E_2{\cdot}k_{16} + k_{13}{\cdot}E_2{\cdot}k_7{\cdot}k_{10} + k_{13}{\cdot}E_2{\cdot}k_7{\cdot}k_{11}{\cdot}E_2}{D} \tag{3.44}$$

The red cross sign in numerator means this formation to enzymatic species is not present because of an irreversible reaction. The denominator, D, is the sum of all numerators. In this case, it is the sum of numerators of Eq.3.41, Eq.3.42, Eq.3.43 and Eq.3.44, i.e.,

$$\begin{aligned} D = {} & k_{14}{\cdot}k_{10}{\cdot}k_{12} + k_{15}{\cdot}E_1{\cdot}k_{12}{\cdot}k_{10} + k_{11}{\cdot}E_2{\cdot}k_{16}{\cdot}k_{14} + k_{16}{\cdot}k_{14}{\cdot}k_{10} + k_7{\cdot}k_{14}{\cdot}k_{10} \\ & + k_{11}{\cdot}E_2{\cdot}k_{15}{\cdot}E_1{\cdot}k_7 + k_{10}{\cdot}k_{15}{\cdot}E_1{\cdot}k_7 + k_{14}{\cdot}k_{11}{\cdot}E_2{\cdot}k_7 + k_{14}{\cdot}k_9{\cdot}E_1{\cdot}k_{12} \\ & + k_9{\cdot}E_1{\cdot}k_{12}{\cdot}k_{15}{\cdot}E_1 + k_{13}{\cdot}E_2{\cdot}k_{15}{\cdot}E_1{\cdot}k_{12} + k_{16}{\cdot}k_{14}{\cdot}k_9{\cdot}E_1 + k_{14}{\cdot}k_7{\cdot}k_9{\cdot}E_1 \\ & + k_{15}{\cdot}E_1{\cdot}k_7{\cdot}k_9{\cdot}E_1 + k_{14}{\cdot}k_9{\cdot}E_1{\cdot}k_{11}{\cdot}E_2 + k_9{\cdot}E_1{\cdot}k_{11}{\cdot}E_2{\cdot}k_{15}{\cdot}E_1 + k_{13}{\cdot}E_2{\cdot}k_{15}{\cdot}E_1{\cdot}k_{11}{\cdot}E_2 \\ & + k_{10}{\cdot}k_{13}{\cdot}E_2{\cdot}k_{15}{\cdot}E_1 + k_{13}{\cdot}E_2{\cdot}k_{10}{\cdot}k_{12} + k_{16}{\cdot}k_{13}{\cdot}E_2{\cdot}k_{10} + k_{13}{\cdot}E_2{\cdot}k_{16}{\cdot}k_{11}{\cdot}E_1 \\ & + k_{10}{\cdot}k_{13}{\cdot}E_2{\cdot}k_{16} + k_{13}{\cdot}E_2{\cdot}k_7{\cdot}k_{10} + k_{13}{\cdot}E_2{\cdot}k_7{\cdot}k_{11}{\cdot}E_2 \end{aligned} \tag{3.45}$$

And finally, the steady state velocity v can be written

$$\begin{aligned} v_{K-A,ss}^{random} &= k_7 \cdot (E_1 \cdot Ez \cdot E_2) \\ &= k_7 \cdot \frac{k_{14} \cdot k_9 \cdot E_1 \cdot k_{11} \cdot E_2 + k_9 \cdot E_1 \cdot k_{11} \cdot E_2 \cdot k_{15} \cdot E_1 + k_{13} \cdot E_2 \cdot k_{15} \cdot E_1 \cdot k_{11} \cdot E_2}{D} \\ &\quad \frac{+k_{10} \cdot k_{13} \cdot E_2 \cdot k_{15} \cdot E_1}{D} \cdot (Ez_{tot}) \end{aligned} \tag{3.46}$$

Motif 5 dual-E controller with compulsory order ternary complex mechanism E_1 binding first to Ez

Fig.3.9 is the scheme of motif 5 dual-E controller with compulsory order ternary complex mechanism. In this case, manipulated variable E_1 binds first to Ez, then E_2 binds with $E_1 \cdot Ez$ to form the ternary complex, $E_1 \cdot Ez \cdot E_2$.

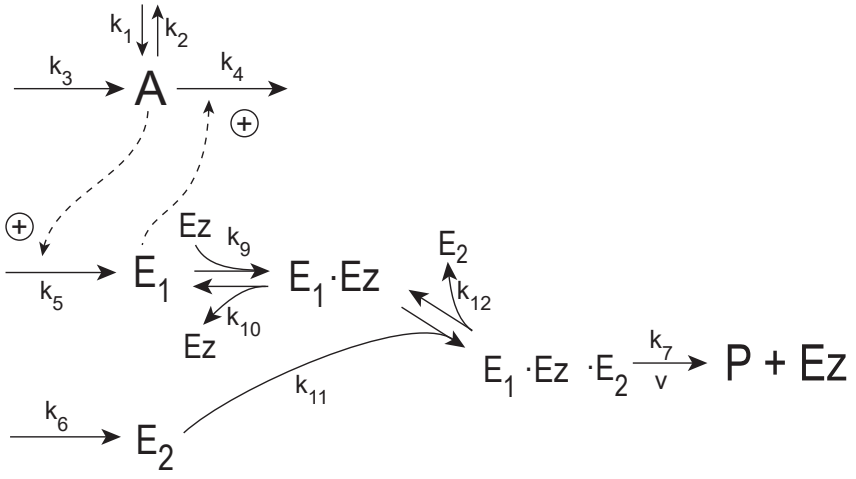

FIGURE 3.9: Motif 5 dual-E controller: removal of E_1 and E_2 by enzyme Ez using a ternary complex mechanism with compulsory order when E_1 binds first to Ez.

The rate equations are

$$\dot{A} = k_1 - k_2 \cdot A + k_3 - k_4 \cdot E_1 \cdot A \tag{3.47}$$

$$\dot{E_1} = k_5 \cdot A - k_9 \cdot E_1 \cdot Ez + k_{10} \cdot (E_1 \cdot Ez) \tag{3.48}$$

$$\dot{E_2} = k_6 - k_{11} \cdot E_2 \cdot (E_1 \cdot Ez) + k_{12} \cdot (E_1 \cdot Ez \cdot E_2) \tag{3.49}$$

$$\dot{Ez} = -k_9 \cdot E_1 \cdot Ez + k_{10} \cdot (E_1 \cdot Ez) + k_7 \cdot (E_1 \cdot Ez \cdot E_2) \tag{3.50}$$

$$\frac{d(E_1 \cdot Ez)}{dt} = k_9 \cdot E_1 \cdot Ez - k_{10} \cdot (E_1 \cdot Ez) - k_{11} \cdot (E_1 \cdot Ez) \cdot E_2 + k_{12} \cdot (E_1 \cdot Ez \cdot E_2) \tag{3.51}$$

$$\frac{d(E_1{\cdot}Ez{\cdot}E_2)}{dt} = k_{11}{\cdot}(E_1{\cdot}Ez){\cdot}E_2 - k_{12}{\cdot}(E_1{\cdot}Ez{\cdot}E_2) - k_7{\cdot}(E_1{\cdot}Ez{\cdot}E_2) \tag{3.52}$$

The velocity for rapid equilibrium assumption using a same method in the random order mechanism above

$$v_{rapid\_eq}^{comp-E_1} = \frac{V_{max}}{(1+\frac{K_{M2}}{(E_2)}+\frac{K_{M1}{\cdot}K_{M2}}{(E_1){\cdot}(E_2)})} \tag{3.53}$$

As for the compulsory order ternary complex mechanism, K_{M1}, K_{M2}, K_{M3} and K_{M4} should also comply with the principle (Eq.3.37). All the enzymatic catalyzed antithetic controllers in this thesis will follow the principle of *detailed balance*.

Fig.3.10 is the scheme of motif 5 dual-E controller under compulsory order ternary complex mechanism E_1 binding first using the King-Altman steady state method.

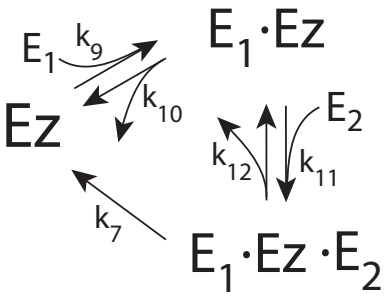

FIGURE 3.10: The scheme of motif 5 dual-E controller under compulsory order when E_1 binds first to Ez using the King-Altman method. The three enzymatic species are arranged in form of a triangle.

Then, the ratio of enzymatic species Ez/Ez_{tot} is

$$\begin{aligned}\frac{\mathrm{Ez}}{\mathrm{Ez_{tot}}} &= \frac{\nwarrow + \uparrow + \swarrow}{D} \\ &= \frac{k_{12}{\cdot}k_{10} + k_{11}{\cdot}E_2{\cdot}k_7 + k_{10}{\cdot}k_7}{D}\end{aligned} \tag{3.54}$$

For enzymatic species $E_1{\cdot}Ez$

$$\begin{aligned}\frac{(\mathrm{E_1{\cdot}Ez})}{\mathrm{Ez_{tot}}} &= \frac{\nwarrow + \not{\uparrow} + \swarrow}{D} \\ &= \frac{k_9{\cdot}E_1{\cdot}k_{12} + k_9{\cdot}E_1{\cdot}k_7}{D}\end{aligned} \tag{3.55}$$

For enzymatic species $E_1{\cdot}Ez{\cdot}E_2$

$$\frac{(\mathrm{E_1{\cdot}Ez{\cdot}E_2})}{\mathrm{Ez_{tot}}} = \frac{\quad + \quad + \quad}{D} = \frac{k_9{\cdot}E_1{\cdot}k_{11}{\cdot}E_2}{D} \tag{3.56}$$

Finally, the steady state velocity is

$$v_{K-A,ss}^{comp-E_1} = k_7{\cdot}\frac{k_9{\cdot}E_1{\cdot}k_{11}{\cdot}E_2}{D}{\cdot}Ez_{tot} \tag{3.57}$$

Motif 5 dual-E controller with compulsory order ternary complex mechanism E_2 binding first to Ez

Fig.3.11 is the scheme of motif 5 dual-E controller with compulsory order ternary complex mechanism. In this case, manipulated variable E_2 binds first to Ez, then E_1 binds with $Ez{\cdot}E_2$ and forms a ternary complex, $E_1{\cdot}Ez{\cdot}E_2$.

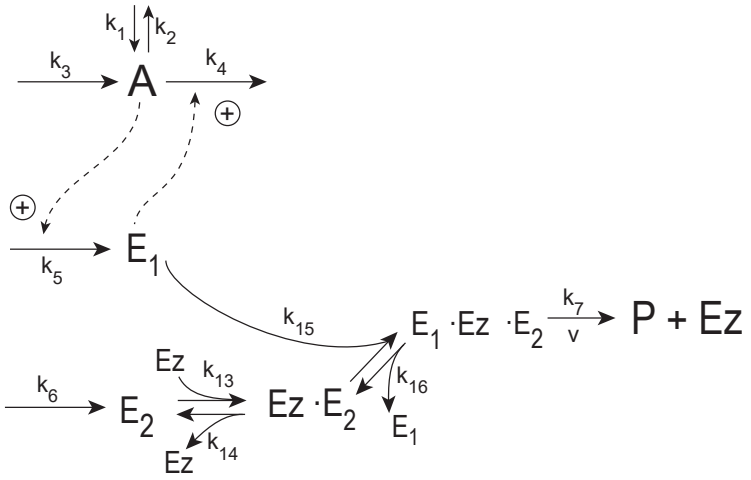

FIGURE 3.11: Motif 5 dual-E controller: removal of E_1 and E_2 by enzyme Ez using a ternary complex mechanism with compulsory order when E_2 binds first to Ez.

The rate equations are

$$\dot{A} = k_1 - k_2{\cdot}A + k_3 - k_4{\cdot}E_1{\cdot}A \tag{3.58}$$

$$\dot{E_1} = k_5{\cdot}A - k_{15}{\cdot}(Ez{\cdot}E_2){\cdot}E_1 + k_{16}{\cdot}(E_1{\cdot}Ez{\cdot}E_2) \tag{3.59}$$

$$\dot{E_2} = k_6 - k_{13}{\cdot}E_2{\cdot}Ez + k_{14}{\cdot}(Ez{\cdot}E_2) \tag{3.60}$$

$$\dot{Ez} = k_7 \cdot (E_1 \cdot Ez \cdot E_2) - k_{13} \cdot Ez \cdot E_2 + k_{14} \cdot (Ez \cdot E_2) \tag{3.61}$$

$$\frac{d(E_1 \cdot Ez \cdot E_2)}{dt} = -k_7 \cdot (E_1 \cdot Ez \cdot E_2) + k_{15} \cdot (Ez \cdot E_2) \cdot E_1 - k_{16} \cdot (E_1 \cdot Ez \cdot E_2) \tag{3.62}$$

$$\frac{d(Ez \cdot E_2)}{dt} = k_{13} \cdot E_2 \cdot Ez - k_{14} \cdot (Ez \cdot E_2) - k_{15} \cdot (Ez \cdot E_2) \cdot E_1 + k_{16} \cdot (E_1 \cdot Ez \cdot E_2) \tag{3.63}$$

The velocity using a rapid equilibrium assumption is

$$v_{rapid\_eq}^{comp-E_2} = \frac{V_{max}}{(1 + \frac{K_{M4}}{(E_1)} + \frac{K_{M3} \cdot K_{M4}}{(E_1) \cdot (E_2)})} \tag{3.64}$$

By applying the King-Altman steady state method, Fig.3.12 is the scheme of motif 5 dual-E controller under compulsory order ternary complex mechanism when E_2 binds first to Ez.

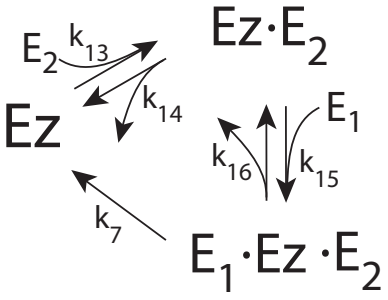

FIGURE 3.12: The scheme of motif 5 dual-E controller under compulsory order when E_2 binds first to Ez using the King-Altman method. Enzymatic species are placed in form of a triangle.

For the ratio of each enzymatic species

$$\frac{\mathrm{Ez}}{\mathrm{Ez_{tot}}} = \frac{\text{ 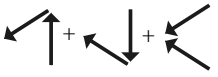 }}{D} = \frac{k_{16} \cdot k_{14} + k_7 \cdot k_{15} \cdot E_1 + k_{14} \cdot k_7}{D} \tag{3.65}$$

$$\frac{(\mathrm{Ez \cdot E_2})}{\mathrm{Ez_{tot}}} = \frac{\text{ 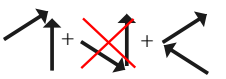 }}{D} = \frac{k_{13} \cdot E_2 \cdot k_{16} + k_7 \cdot k_{13} \cdot E_2}{D} \tag{3.66}$$

$$\frac{(\mathrm{E_1{\cdot}Ez{\cdot}E_2})}{\mathrm{Ez_{tot}}} = \frac{\quad + \quad + \quad}{D} = \frac{k_{13}{\cdot}E_2{\cdot}k_{15}{\cdot}E_1}{D} \tag{3.67}$$

Thus, the steady state velocity is

$$v_{K-A,ss}^{comp-E_2} = k_7{\cdot}\frac{k_{13}{\cdot}E_2{\cdot}k_{15}{\cdot}E_1}{D}{\cdot}Ez_{tot} \tag{3.68}$$

Motif 5 dual-E controller with substitution (ping-pong) mechanism E_1 binding first to Ez

Fig.3.13 is the scheme of motif 5 dual-E controller using a ping-pong mechanism. In this case, the enzyme Ez binds first with E_1 to release an actived Ez^*. Then E_2 comes to substitution binding with Ez^* to generate the final product, P.

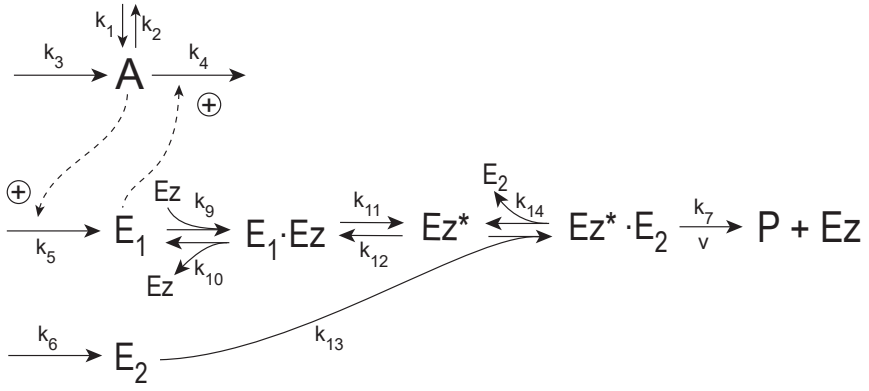

FIGURE 3.13: Motif 5 dual-E controller: removal of E_1 and E_2 by enzyme Ez using a ping-pong mechanism when E_1 binds first to Ez.

The rate equations are

$$\dot{A} = k_1 - k_2{\cdot}A + k_3 - k_4{\cdot}E_1{\cdot}A \tag{3.69}$$

$$\dot{E_1} = k_5{\cdot}A - k_9{\cdot}E_1{\cdot}Ez + k_{10}{\cdot}(E_1{\cdot}Ez) \tag{3.70}$$

$$\dot{E_2} = k_6 - k_{13}{\cdot}E_2{\cdot}Ez^* + k_{14}{\cdot}(Ez^*{\cdot}E_2) \tag{3.71}$$

$$\dot{Ez} = -k_9{\cdot}E_1{\cdot}Ez + k_{10}{\cdot}(E_1{\cdot}Ez) + k_7{\cdot}(Ez^*{\cdot}E_2) \tag{3.72}$$

$$\frac{d(E_1{\cdot}Ez)}{dt} = k_9{\cdot}E_1{\cdot}Ez - k_{10}{\cdot}(E_1{\cdot}Ez) - k_{11}{\cdot}(E_1{\cdot}Ez) + k_{12}{\cdot}Ez^* \tag{3.73}$$

$$\frac{d(Ez^*{\cdot}E_2)}{dt} = k_{13}{\cdot}E_2{\cdot}Ez^* - k_{14}{\cdot}(Ez^*{\cdot}E_2) - k_7{\cdot}(Ez^*{\cdot}E_2) \tag{3.74}$$

$$\frac{d(Ez^*)}{dt} = k_{11}{\cdot}(E_1{\cdot}Ez) - k_{12}{\cdot}Ez^* - k_{13}{\cdot}E_2{\cdot}Ez^* + k_{14}{\cdot}(Ez^*{\cdot}E_2) \tag{3.75}$$

The derivation of velocity using a rapid equilibrium assumption are

$$K_{M1} = \frac{(E_1){\cdot}(Ez)}{(E_1{\cdot}Ez)} = \frac{k_{10}}{k_9} \tag{3.76}$$

$$K_{M2} = \frac{(E_1{\cdot}Ez^*)}{(Ez^*)} = \frac{k_{12}}{k_{11}} \tag{3.77}$$

$$K_{M3} = \frac{(Ez^*){\cdot}(E2)}{(Ez^*{\cdot}E_2)} = \frac{k_{14}}{k_{13}} \tag{3.78}$$

Since

$$v = k_7{\cdot}(Ez^*{\cdot}E_2) \tag{3.79}$$

that we have

$$Ez_{tot} = (Ez) + (E_1{\cdot}Ez) + (Ez^*{\cdot}E_2) + (Ez^*) \tag{3.80}$$

$$(Ez^*) = \frac{K_{M3}}{(E_2)}{\cdot}(Ez^*{\cdot}E_2) \tag{3.81}$$

$$(E_1{\cdot}Ez) = K_{M2}{\cdot}(Ez^*) = \frac{K_{M2}{\cdot}K_{M3}}{(E_2)}{\cdot}(Ez^*{\cdot}E_2) \tag{3.82}$$

$$(Ez) = \frac{K_{M1}}{(E_1)}{\cdot}(E_1{\cdot}Ez) = \frac{K_{M1}{\cdot}K_{M2}{\cdot}K_{M3}}{(E_1){\cdot}(E_2)}{\cdot}(Ez^*{\cdot}E_2) \tag{3.83}$$

$$\begin{aligned} \mathrm{Ez_{tot}} &= (\frac{K_{M1}{\cdot}K_{M2}{\cdot}K_{M3}}{(E_1){\cdot}(E_2)} + \frac{K_{M2}{\cdot}K_{M3}}{(E_2)} + \frac{K_{M3}}{(E_2)} + 1){\cdot}(Ez^*{\cdot}E_2) \\ &= (\frac{K_{M1}{\cdot}K_{M2}{\cdot}K_{M3}}{(E_1){\cdot}(E_2)} + \frac{K_{M3}{\cdot}(1{+}K_{M2})}{(E_2)} + 1){\cdot}(Ez^*{\cdot}E_2) \\ &= (1{+}\frac{\alpha}{(E_2)}{+}\frac{\beta}{(E_1){\cdot}(E_2)}){\cdot}(Ez^*{\cdot}E_2) \end{aligned} \tag{3.84}$$

Finally,

$$v_{rapid\_eq}^{PP-E_1} = \frac{k_7{\cdot}Ez_{tot}}{(1{+}\frac{\alpha}{(E_2)}{+}\frac{\beta}{(E_1){\cdot}(E_2)})} = \frac{V_{max}}{(1{+}\frac{\alpha}{(E_2)}{+}\frac{\beta}{(E_1){\cdot}(E_2)})} \tag{3.85}$$

Note that, $\alpha{=}K_{M3}{\cdot}(1{+}K_{M2})$ and $\beta{=}K_{M1}{\cdot}K_{M2}{\cdot}K_{M3}$.

Fig.3.14 is the scheme of motif 5 dual-E controller under ping-pong mechanism E_1 binding first to Ez using the King-Altman steady state method.

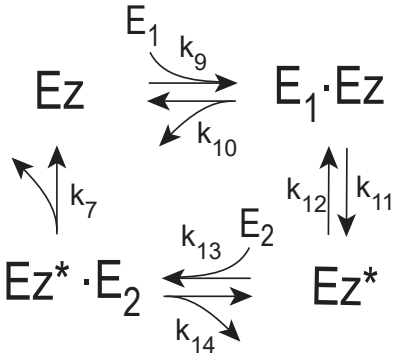

FIGURE 3.14: The scheme of motif 5 dual-E controller with a ping-pong mechanism when E_1 binds first to Ez using the King-Altman method. Enzymatic species are arranged in form of a square.

For the ratio of each enzymatic species

$$\frac{\mathrm{Ez}}{\mathrm{Ez_{tot}}} = \frac{\quad + \quad + \quad + \quad}{D} = \frac{k_7{\cdot}k_{10}{\cdot}k_{12} + k_{14}{\cdot}k_{12}{\cdot}k_{10} + k_{11}{\cdot}k_{13}{\cdot}E_2{\cdot}k_7 + k_{13}{\cdot}E_2{\cdot}k_7{\cdot}k_{10}}{D} \tag{3.86}$$

$$\frac{(\mathrm{E_1{\cdot}Ez})}{\mathrm{Ez_{tot}}} = \frac{\quad + \quad + \quad + \quad}{D} = \frac{k_7{\cdot}k_9{\cdot}E_1{\cdot}k_{12} + k_{14}{\cdot}k_{12}{\cdot}k_9{\cdot}E_1 + k_{13}{\cdot}E_2{\cdot}k_7{\cdot}k_9{\cdot}E_1}{D} \tag{3.87}$$

$$\frac{(\mathrm{Ez^*})}{\mathrm{Ez_{tot}}} = \frac{\quad + \quad + \quad + \quad}{D} = \frac{k_7{\cdot}k_9{\cdot}E_1{\cdot}k_{11} + k_9{\cdot}E_1{\cdot}k_{11}{\cdot}k_{14}}{D} \tag{3.88}$$

$$\frac{(\mathrm{Ez^*{\cdot}E_2})}{\mathrm{Ez_{tot}}} = \frac{\quad + \quad + \quad + \quad}{D} = \frac{k_9{\cdot}E_1{\cdot}k_{11}{\cdot}k_{13}{\cdot}E_2}{D} \tag{3.89}$$

Finally, the steady state velocity is

$$v_{K-A,ss}^{PP-E_1} = k_7 \cdot \frac{k_9 \cdot E_1 \cdot k_{11} \cdot k_{13} \cdot E_2}{D} \cdot Ez_{tot} \tag{3.90}$$

Motif 5 dual-E controller with substitution (ping-pong) mechanism E_2 binding first to Ez

Fig.3.13 is the scheme of motif 5 dual-E controller with ping-pong mechanism. In this case, the free enzyme Ez binds with E_2 first to release an actived Ez^*. Then E_1 comes to substitution binding with Ez^* to generate the final product, P.

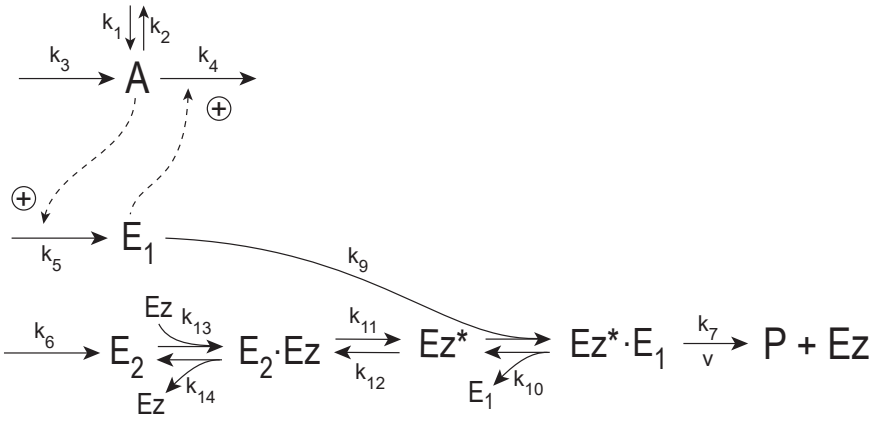

FIGURE 3.15: Motif 5 dual-E controller: removal of E_1 and E_2 by enzyme Ez using a ping-pong mechanism when E_2 binds first to Ez.

The rate equations are

$$\dot{A} = k_1 - k_2 \cdot A + k_3 - k_4 \cdot E_1 \cdot A \tag{3.91}$$

$$\dot{E_1} = k_5 \cdot A - k_9 \cdot E_1 \cdot Ez^* + k_{10} \cdot (Ez^* \cdot E_1) \tag{3.92}$$

$$\dot{E_2} = k_6 - k_{13} \cdot E_2 \cdot Ez + k_{14} \cdot (E_2 \cdot Ez) \tag{3.93}$$

$$\dot{Ez} = -k_{13} \cdot E_2 \cdot Ez + k_{14} \cdot (E_2 \cdot Ez) + k_7 \cdot (Ez^* \cdot E_1) \tag{3.94}$$

$$\frac{d(E_2 \cdot Ez)}{dt} = k_{13} \cdot E_2 \cdot Ez - k_{14} \cdot (E_2 \cdot Ez) - k_{11} \cdot (E_2 \cdot Ez) + k_{12} \cdot Ez^* \tag{3.95}$$

$$\frac{d(Ez^* \cdot E_1)}{dt} = k_9 \cdot E_1 \cdot Ez^* - k_{10} \cdot (Ez^* \cdot E_1) - k_7 \cdot (Ez^* \cdot E_1) \tag{3.96}$$

$$\frac{d(Ez^*)}{dt} = k_{11} \cdot (E_2 \cdot Ez) - k_{12} \cdot Ez^* - k_9 \cdot E_1 \cdot Ez^* + k_{10} \cdot (Ez^* \cdot E_1) \tag{3.97}$$

The velocity using a rapid equilibrium assumption is

$$v_{rapid\_eq}^{PP-E_2} = \frac{V_{max}}{(1+\frac{\alpha}{(E_1)}+\frac{\beta}{(E_1)\cdot(E_2)})} \tag{3.98}$$

Note that, α=K_{M1}·(1+K_{M2}) and β=K_{M1}·K_{M2}·K_{M3}.

Fig.3.16 is the scheme of motif 5 dual-E controller under ping-pong mechanism E_2 binding first using King-Altman steady state method.

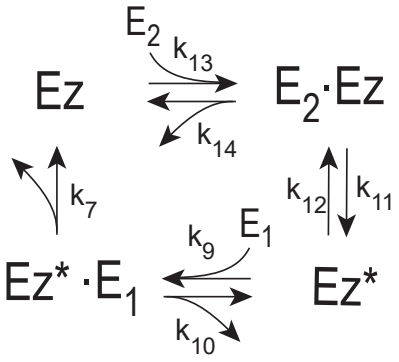

FIGURE 3.16: The scheme of motif 5 dual-E controller with a ping-pong mechanism when E_2 binds first using the King-Altman method. The four enzymatic species are arranged in form of a square.

For the ratios of each enzymatic species are:

$$\frac{\mathrm{Ez}}{\mathrm{Ez_{tot}}} = \frac{\uparrow\uparrow + \rightleftarrows + \uparrow\downarrow + \leftarrow\leftarrow}{D} = \frac{k_{14}\cdot k_{12}\cdot k_7 + k_{14}\cdot k_{12}\cdot k_{10} + k_7\cdot k_9\cdot E_1\cdot k_{11} + k_{14}\cdot k_7\cdot k_9\cdot E_1}{D} \tag{3.99}$$

$$\frac{(\mathrm{E_2{\cdot}Ez})}{\mathrm{Ez_{tot}}} = \frac{\uparrow\uparrow + \rightleftarrows + \not\uparrow\not\downarrow + \leftarrow\leftarrow}{D} = \frac{k_{13}\cdot E_2\cdot k_7\cdot k_{12} + k_{13}\cdot E_2\cdot k_{12}\cdot k_{10} + k_7\cdot k_9\cdot E_1\cdot k_{13}\cdot E_2}{D} \tag{3.100}$$

$$\frac{(\mathrm{Ez^*})}{\mathrm{Ez_{tot}}} = \frac{\uparrow\downarrow + \rightleftarrows + \not\rightleftarrows + \not\leftarrow\not\rightarrow}{D} = \frac{k_7\cdot k_{13}\cdot E_2\cdot k_{11} + k_{13}\cdot E_2\cdot k_{11}\cdot k_{10}}{D} \tag{3.101}$$

$$\frac{(\mathrm{Ez}^{*}\cdot \mathrm{E}_1)}{\mathrm{Ez}_{\mathrm{tot}}} = \frac{\quad + \quad + \quad + \quad}{D} = \frac{k_{13}\cdot E_2 \cdot k_{11}\cdot k_9 \cdot E_1}{D} \tag{3.102}$$

Finally, the steady state velocity is

$$v_{K-A,ss}^{PP-E_2} = k_7 \cdot \frac{k_{13}\cdot E_2 \cdot k_{11}\cdot k_9 \cdot E_1}{D} \cdot Ez_{tot} \tag{3.103}$$

Comparing the catalyzed motif 5 controllers: set point defence and enzyme limitation

In this case, the single-E controller is compared with all five kinds of dual-E controllers, which described above, and finally six controllers in total. In the figure, the single-E controller is in cyan and dual-E controllers are: in blue, random order ternary complex mechanism; in red, compulsory order E_1 binding first; in black, compulsory order E_2 binding first; in green, ping-pong mechanism E_1 binding first; in purple, ping-pong mechanism E_2 binding first. Labels are shown in the bottom of Fig.3.17.

In order to make things simple, the non zero-order condition is defined by a low perturbation, k_1, as discussed before.

In Fig.3.17, the left column (**1**-**3**) is under non zero-order condition with a small perturbation, while the right column (**4**-**6**) is under zero-order condition with a relatively large perturbation. As for **2**-**3** and **5**-**6**, the all of five kinds of the dual-E controllers can arrive at its set point with the low value of k_6 no matter in a non zero-order or a zero-order condition, while the single-E controller worked well in zero-order condition but had a off-set from its set point in non zero-order condition. An interesting behavior for dual-E controllers in **2**, there is a transition moving A from $A_{ss}^{single-E}$ to A_{ss}^{dual-E} and same transition can be observed in **5** but no in **3** and **6**. The only difference between **2** and **3**, and between **5** and **6** is the initial concentration of E_2 is much lower in **3** and **6** than in **2** and **5**, respectively.

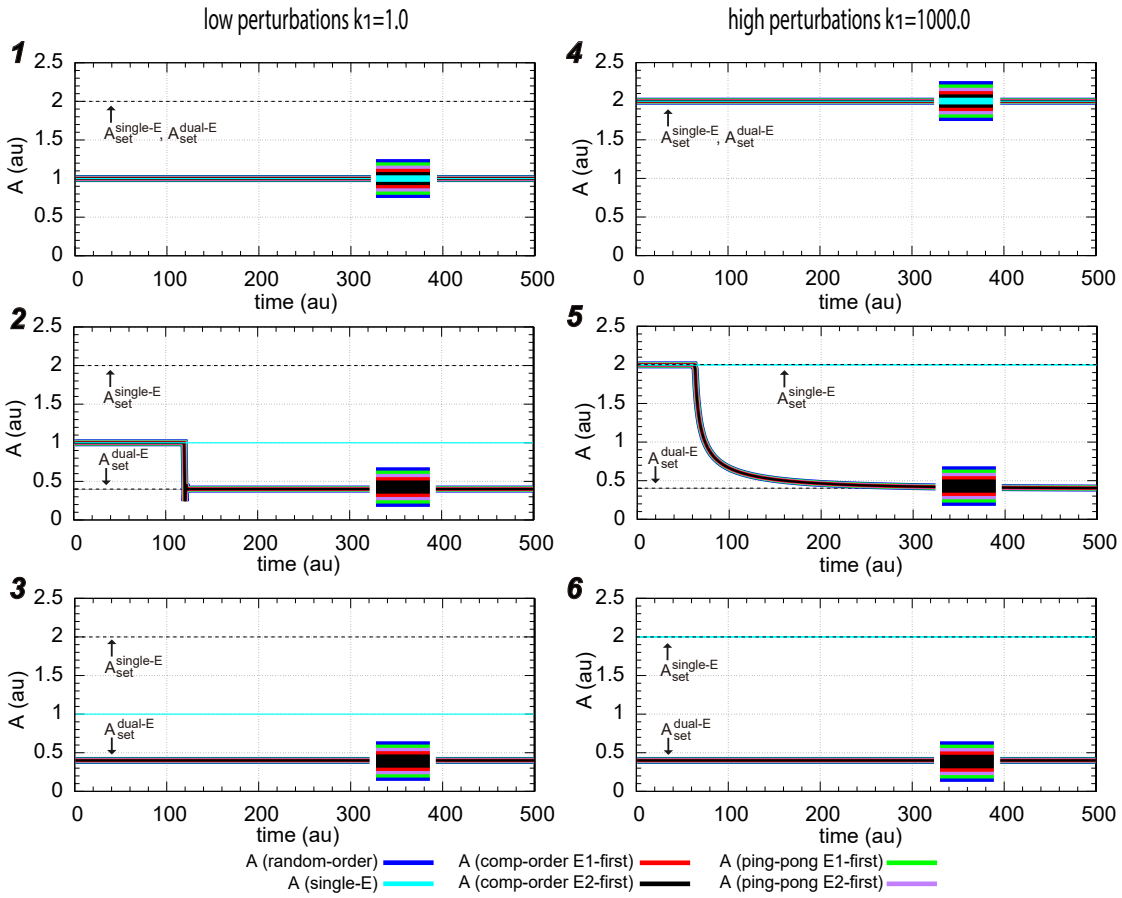

FIGURE 3.17: The comparison of motif 5 single-E and dual-E controllers to defend their set point. Perturbation: **1-3**, k_1=1.0; **4-6**, k_1=1000.0. Rate constants: k_2=1.0, k_3=0.0, k_4=1.0, $k_5 = 50$, $k_7 = 10^{+5}$, $k_8 = 0.1$, k_9=1×10^{+9}, k_{10}=1×10^{+3}, k_{11}=1×10^{+9}, k_{12}=1×10^{+3}, k_{13}=1×10^{+9}, k_{14}=1×10^{+3}, k_{15}=1×10^{+9}, k_{16}=1×10^{+3}, Ez_{tot}=1×10^{-3}. For **1** and **4**, k_6=10^{+3} with the set point A_{set}^{dual-E}=20.0 while $A_{set}^{single-E}$=2.0. For the rest **2**, **3**, **5** and **6**, k_6=20 with the set point $A_{set}^{single-E}$=2.0 and A_{set}^{dual-E}=0.4 respectively. In parallel, a set of Matlab programs are in Appendix for verification and further exploration.

This kind of transition is illustrated by using Fig.3.18 (**c**) and (**d**). As for Fig.3.18 (**c**), it is the behavior of controller species from Fig.3.17 (**2**) and Fig.3.18 (**d**) is from Fig.3.17 (**3**). In Fig.3.18 (**c**), it can be seen that E_2 decreased for some times then equaling about zero and it is the time when E_2 equal to zero that E_1 increased. During the decrease of E_2, the value of E_2 is quite large compared with E_1, that is why the dual-E controllers have a set point at $A_{ss}^{single-E}$. It is the time, when the value of E_2 is near zero, E_1 increased and is relative large comparing with E_2, the switch occur moving A to A_{set}^{dual-E} corresponding to Fig.3.17 (**2**). When focusing on Fig.3.18 (**d**), the value of E_2 is much lower than E_1 from the beginning. Thus, dual-E controllers arrive at its set point at very beginning in Fig.3.17 (**3**). The same is true for Fig.3.17 (**5**) and (**6**).

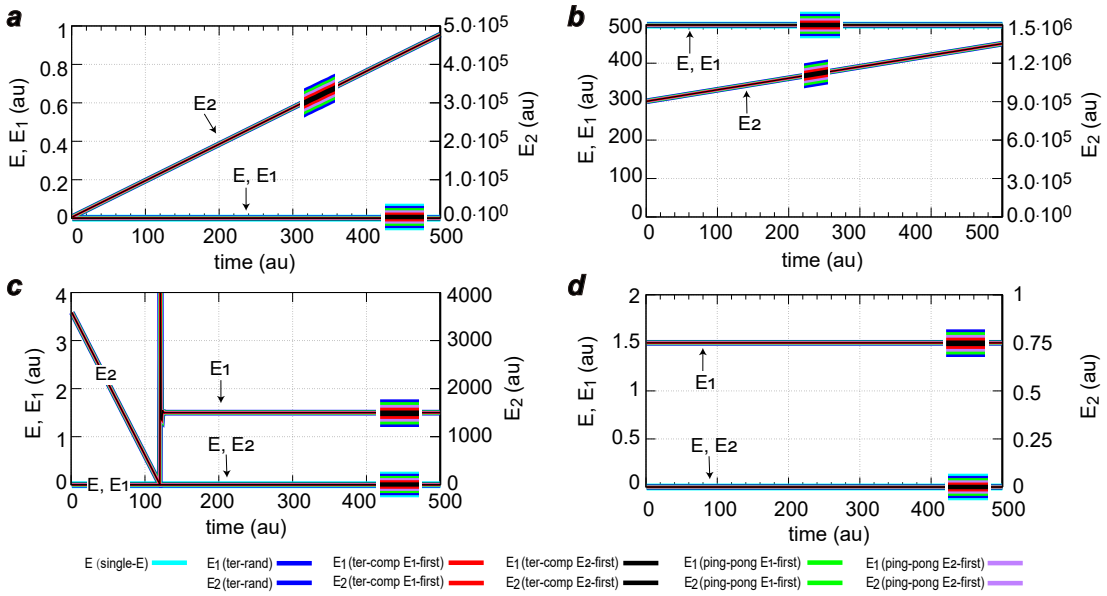

FIGURE 3.18: The behavior of controller species E, E_1 and E_2 in single-E and dual-E controllers. (**a**) The controller species from Fig.3.17 (**1**). (**b**) The controller species from Fig.3.17 (**4**). (**c**) The controller species from Fig.3.17 (**2**). (**d**) The controller species from Fig.3.17 (**3**).

As for Fig.3.17 (**1**) and (**4**), single-E controller can defend its set point in zero-order condition but fail in non zero-order conditions. And for the dual-E controllers, all fail to get the set point (20.0) both in zero-order and non zero-order conditions. It is noteworthy that the A value of dual-E controllers are equal to the single-E one. The reasons are as follow using Fig.3.18 (**a**) and (**b**) for explanation. In Fig.3.18 (**a**), we can see E_2 species increase all the time while E_1 species keep constant near zero, which means a large value of E_2 keep consuming E_1 leading to little amount of E_1 working to defend its set point. Eventually, an off-set occurs. On the other hand, the E_2 species play no role on the regulation in negative feedback loop, which means only the E_1 specie participates in regulation and the dual-E controllers work just like the single-E controller as shown in Fig.3.20 (**e**). Thus, A_{dual-E} is equal to $A_{single-E}$ in (**1**), and called dual-E controllers work in a single-E control mode. The same is true for Fig.3.18 (**b**) from Fig.3.17 (**4**). The results above can approve the view before that the set point of a dual-E controller is depended on the concentration of E_2 in comparison with E_1. When E_2 is relative large compared to E_1, dual-E controllers have the same set point as single-E controller, i.e.,

$$A_{set} = \frac{k_7 \cdot Ez_{tot}}{k_5} \tag{3.104}$$

Alternatively, when E_2 is relative low, dual-E controllers have the set point

$$A_{set} = \frac{k_6}{k_5} \tag{3.105}$$

To sum up, the dual-E controllers show a better performance than the single-E controllers, since the dual-E controllers can defend their set points both under zero-order and non zero-order conditions when work in the dual-E control mode. When the dual-E controllers work in the single-E control mode, they have the same behavior of A as for the single-E controllers.

Enzyme limitation

Considering the influence of the enzyme concentration, the comparison is done similar to Fig.3.17 but the total concentration of enzyme was changed from 1×10^{-3} to 1×10^{-6} now. As discussed before, the set point is defined by Eq.3.17, which means when Ez_{tot} is decreased by three order of magnitude to 1×10^{-6}, the value of k_7 should be adjusted correspondingly by three order of magnitude to $1\times10^{+8}$ to have the same A_{set} both in Fig.3.17 and Fig.3.19.

From Fig.3.19, it is easy to see that single-E controller still has an off-set in non zero-order condition but works well in zero-order conditions. As for the dual-E controllers, roughly it is similar to Fig.3.17 defending the set point successfully independent of non zero-order or zero-order conditions. However, focusing on Fig.3.19 (**4**), the behavior of A for ping-pong mechanism E_1/E_2 binding first and compulsory order ternary complex mechanism E_2 binding first have a small off-set different from other dual-E controllers. Actually, in Fig.3.19 (**1**), these three controllers also have a little different from other, when look into details from the program result that the value of A is equaling 0.915 for these three with others equaling 0.921, respectively. But when the value of k_6 is changed becoming smaller (Fig.3.19 **2**, **3**, **5** and **6**), all the dual-E controllers defend its set point well.

Therefore, considering an enzyme limitation, it has a little impact on the dual-E controllers for ping-pong mechanism E_1/E_2 binding first and compulsory order ternary complex mechanism E_2 binding first. Overall, all five dual-E controllers have the ability to defend their set points.

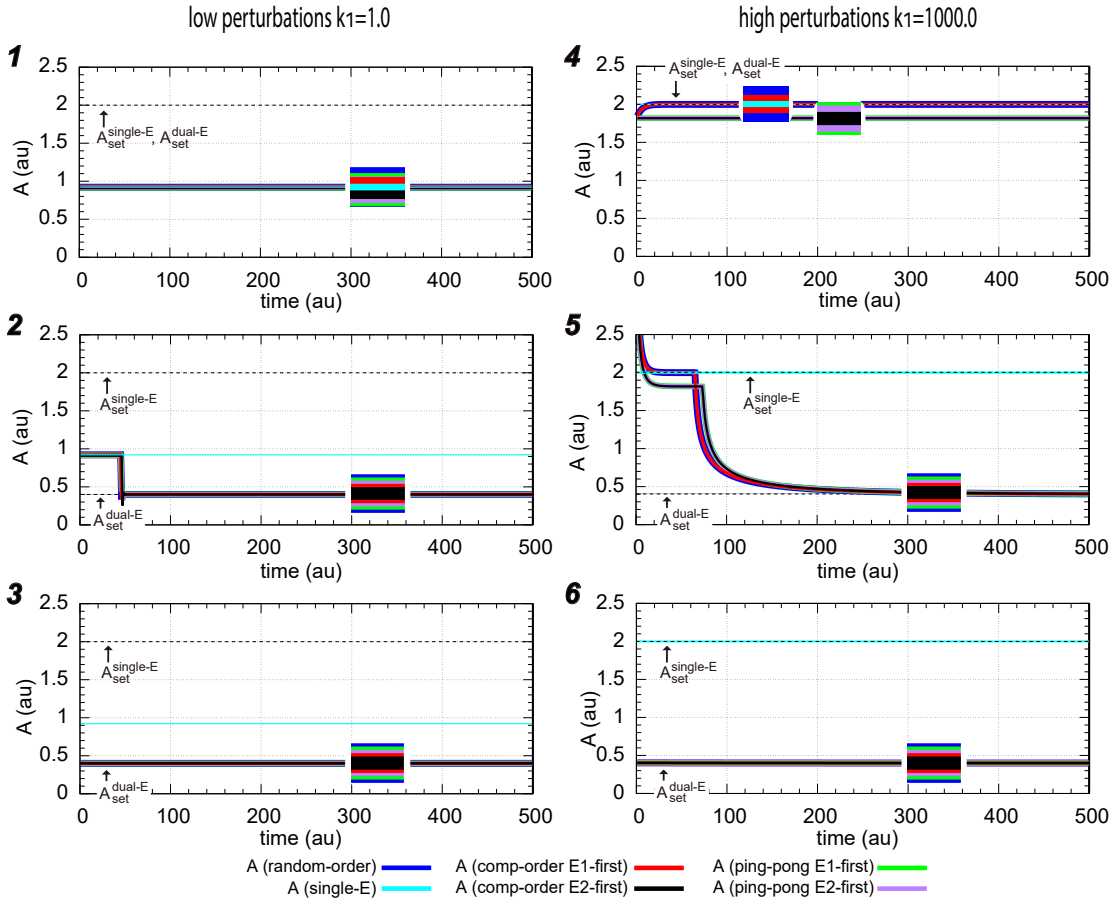

FIGURE 3.19: The comparison of motif 5 single-E and dual-E controllers to defend a set point. Rate constants are same as in Fig.3.17, but k_7=1×10^{+8}, Ez_{tot}=1×10^{-6}.

Switching between dual-E and single-E control mode of motif 5 catalyzed antithetic controllers

The case in motif 5 catalyzed antithetic controller, a switching between dual-E and single-E control mode, can be defined as follow. As the set point can be calculated in two ways, we have the equation

$$A_{set} = \frac{k_6}{k_5} = \frac{k_7 \cdot Ez_{tot}}{k_5} \tag{3.106}$$

As shown in Fig.3.20 (**a**). It is easy to observe when

$$\frac{k_6}{k_5} \geq \frac{k_7 \cdot Ez_{tot}}{k_5} \tag{3.107}$$

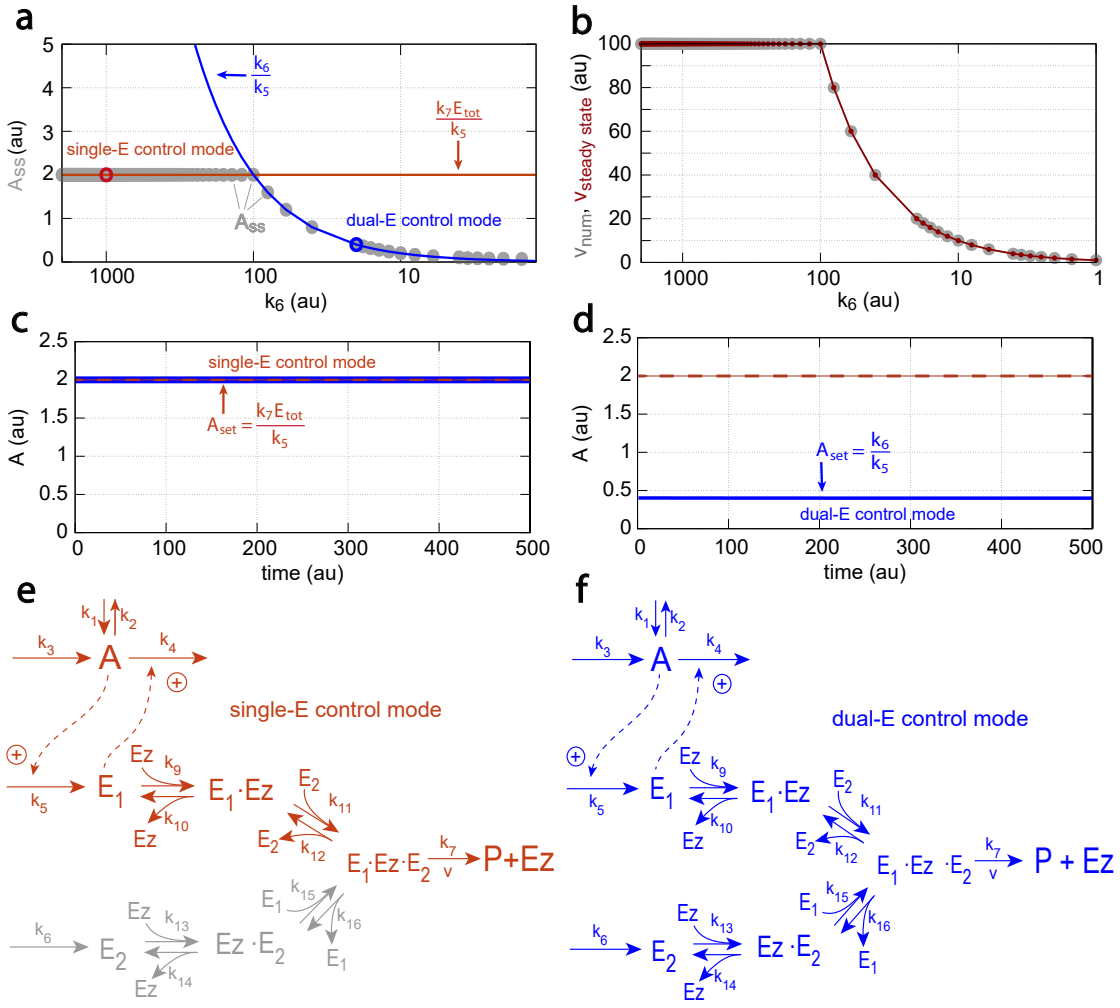

FIGURE 3.20: Switch between single-E and dual-E control mode in motif 5 catalyzed antithetic controller, with random order ternary complex mechanism in the removal of E_1 and E_2. (**a**) A_{ss} as a function of k_6. The A value for single-E and dual-E control mode are shown as red and blue lines, respectively. The gray solid points are the numerically calculated steady state values. The outlined red and blue circles show the k_6 values (1000.0 and 20.0) used in panels **c** and **d**. (**b**) Steady state values of v (Eq.3.46) calculated by King-Altman method (red line) and numerical velocities (gray points). (**c**) and (**d**) Single-E and dual-E control mode with k_6 equaling 1000.0 and 20.0 respectively. They come from Fig.3.17 (**4**) and (**6**) with plotting only the A values for random order ternary complex mechanism. (**e**) The part of the network outlined in red is active during single-E control mode with E_2 continuously increasing. (**f**) The entire network is active during dual-E control mode (outlined in blue).

means $k_7 \cdot Ez_{tot}/k_5$ is dominating (the left part on the red line of Fig.3.20 **a**). Only manipulated variable E_1 is functioning properly, while the values of E_2 is increasing continuously (Fig.3.18 **b**). And then we call dual-E controller works in single-E control mode (Fig.3.20 **c** and **e**).

On the contrary, when

$$\frac{k_6}{k_5} < \frac{k_7 \cdot Ez_{tot}}{k_5} \tag{3.108}$$

means the set point of the dual-E controller will be equal to the value of k_6/k_5 (the right part on the blue line of Fig.3.20 **a**). The dual-E controller works in a general dual-E control mode (Fig.3.20 **d**). As Fig.3.20 (**f**) shows, both E_1 and E_2 take part in the regulation of A.

And the switching not only happens in the zero-order condition (Fig.3.17 (**5**) and Fig.3.19 (**5**)) but also in non zero-order condition (Fig.3.17 (**2**) and Fig.3.19 (**2**)) and has similar behavior as in (Fig.3.20 **a**). However, as discussed before, the single-E controller has an off-set under non zero-order condition thus the same off-set will occur in the level of A_{ss} and we would not display the details here.

Reaction velocity of E_1/E_2 degradation

In order to check whether the program is valid, the reaction velocity of degradation of E_1 and E_2 is calculated by using the King-Altman steady state method and rapid equilibrium assumption and compared with numerical velocity. The value of velocity from steady state always agrees with the numerical one while the rapid equilibrium one is far away, which is in line with expectations. Fig.3.20 (**b**) shows one example that velocity from King-Altman steady state method equal to the numerical one. Here, only the ternary complex random order mechanism is plotted. In fact, this occurs for all five dual-E controllers.

Motif 2 uncatalyzed antithetic integral controller in comparison with zero-order integral controller

In order to compare motif 5-based controllers with motif 2-based controllers, in the following, motif 2 negative feedback loops are introduced and extended to their uncatalyzed versions.

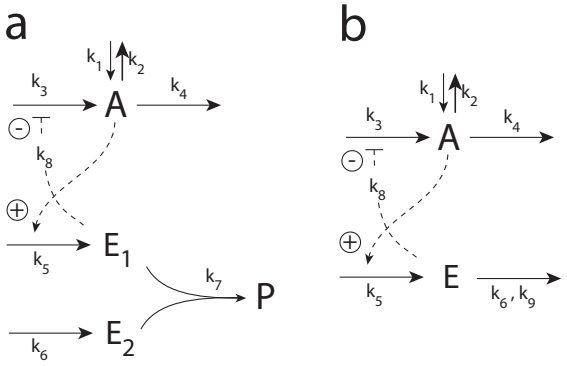

FIGURE 3.21: Scheme of antithetic controller based on motif 2. (**a**) Uncatalyzed antithetic controller based on motif 2. (**b**) Basic inflow controller, motif 2.

Motif 2 is an inflow type of controller compensating outflow perturbation by derepressing the controlled variable A, which differs from motif 5. For Fig.3.21 (**a**), we have the rate equations

$$\dot{A} = k_1 - k_2 \cdot A + \frac{k_3 \cdot k_8}{k_8 + E} - k_4 \cdot E \cdot A \tag{3.109}$$

$$\dot{E_1} = k_5 \cdot A - k_7 \cdot E_1 \cdot E_2 \tag{3.110}$$

$$\dot{E_2} = k_6 - k_7 \cdot E_1 \cdot E_2 \tag{3.111}$$

For Fig.3.21 (**b**), we have the rate equations

$$\dot{A} = k_1 - k_2 \cdot A + \frac{k_3 \cdot k_8}{k_8 + E} - k_4 \cdot E \cdot A \tag{3.112}$$

$$\dot{E} = k_5 \cdot A - \frac{k_6 \cdot E}{k_9 + E} \tag{3.113}$$

When $k_9 \ll E$, the set point, A_{set}, can be written as

$$A_{set} = \frac{k_6}{k_5} \tag{3.114}$$

Different outflow perturbations, k_2, were applied in motif 2-based controllers to understand their performances.

Firstly, with respect to previous findings [5], the motif 2 zero-order integral controller works well not only under step-wise perturbations but also under linearly increasing perturbations. However, the result (Fig.3.22) shows that the uncatalyzed antithetic motif 2 controller can defend its set point with step-wise perturbation (Row **a**) but not with

linearly increasing k_2 values. Row **b** shows the increased off-set with increased $\dot{k_2}$. Both controllers fail with exponentially increasing perturbations (Row **c**).

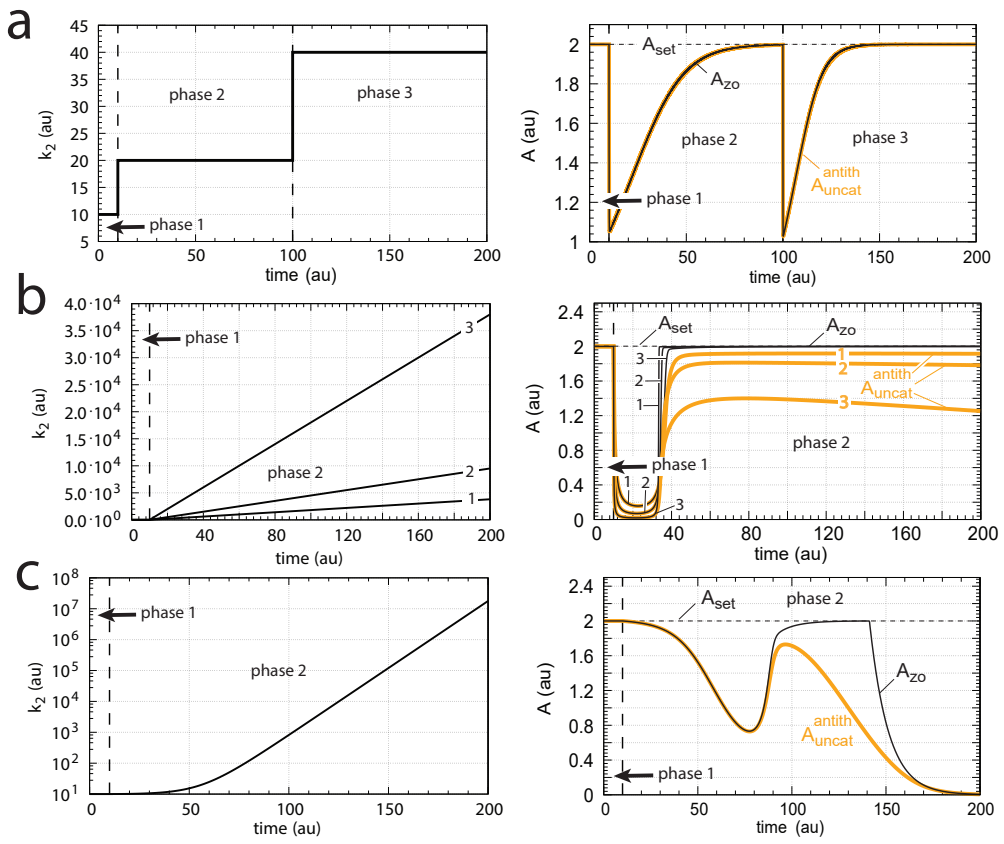

FIGURE 3.22: Comparison between integral motif 2 negative and uncatalyzed antithetic controller. (Row **a**) Step-wise perturbations in k_2; left panel, phase 1 (0-10 time units): k_2=10.0, phase 2 (10-100 time units): k_2=20.0, phase 3 (100-200 time units): k_2=40.0; right panel: behavior of controlled variable A_{zo} for zero-order controller motif 2 in black and controlled variable A_{uncat}^{antith} for uncatalyzed antithetic controller in orange. (Row **b**) Linear increases of k_2; left panel, phase 1 (0-10 time units): k_2 is kept constant at 10.0, phase 2 (10-200 time units): k_2 starts to increase with (1) $\dot{k_2}$=20.0, (2) $\dot{k_2}$=50.0, (3) $\dot{k_2}$=200.0; right panel: behavior of controller variable A_{zo} for zero-order controller in black and A_{uncat}^{antith} for uncatalyzed antithetic controller in orange. (Row **c**) Exponential increase of k_2; left panel, phase 1 (0-10 time units): k_2 is kept constant at 10.0, phase 2 (10-200 time units): k_2 starts to increase according to k_2(t)=10+0.1($e^{[0.1(t-10)]}$-1); right panel, behavior of controlled variable A_{zo} for zero-order controller in black and A_{uncat}^{antith} for uncatalyzed antithetic controller in orange. Rate constants: k_1=0.0, k_3=1×10^{+5}, k_4=1.0, k_5=10.0, k_6=20.0, k_7=0.1, k_8=0.1, k_9=1×10^{-6}.

Controller basing on motif 2: aggressiveness and accuracy

As considering the aggressiveness, a higher aggressiveness will improved the response time.

As for the accuracy, the result (Fig.3.23) shows that the values of A_{ss} for the uncatalyzed antithetic controller (A_{uncat}^{antith}) comes closer to the value of the zero-order single-E controller (A_{zo}) with an increasing k_7.

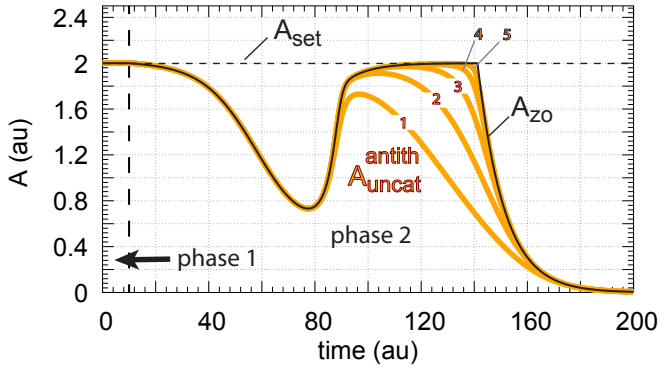

FIGURE 3.23: Comparison of accuracy with increasing k_7 in the uncatalyzed antithetic motif 2 controller. Rate constants are the same as in Fig.3.22 **c**, but with the following changes: 1, k_7=0.1 (unaltered); 2, k_7=1.0; 3, k_7=10.0; 4, k_7=100.0; 5, k_7=1000.0.

The increasing accuracy is because a higher k_7 value leads to a more rapid removal of E_1 and E_2, which means less E_1 could work on the inhibition of A accumulation. Then, more inflow A compensate for the outflow perturbations resulting in an approaching value to A_{zo}.

Motif 2 antithetic controller with enzymatic catalyzed mechanisms

In the following, an explicitly enzyme is included in motif 2-based controller for the degradation of manipulated variables, E and E_1/E_2. Since the results in motif 5-based show that there is no significant difference between the different kinetics within the two-substrate enzyme systems, only ternary complex random order mechanism for dual-E controller of motif 2-based is discussed in this section.

Mechanism of motif 2 catalyzed single-E and dual-E controllers and the rate equations derivation

Firstly, the mechanistic schemes and their rate equations are introduced.

Motif 2 single-E controller with Michaelis-Menten degradation of E

Fig.3.24 shows the scheme of motif 2 single-E controller explicitly including an enzyme using the Michaelis-Menten mechanism.

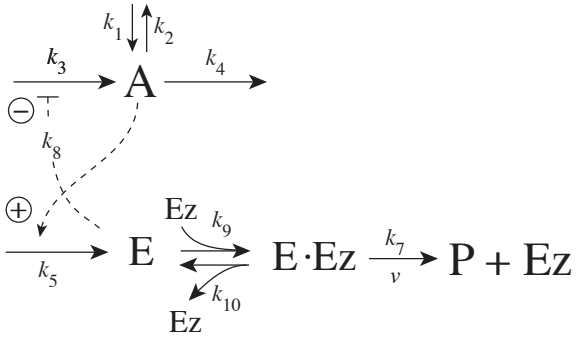

FIGURE 3.24: Motif 2 single-E controller: removal of E by enzyme Ez using a Michaelis-Menten mechanism.

The rate equations are

$$\dot{A} = k_1 - k_2 \cdot A - k_4 \cdot A + \frac{k_3 \cdot k_8}{k_8 + E} \tag{3.115}$$

$$\dot{E} = k_5 \cdot A - k_9 \cdot (E) \cdot (Ez) + k_{10} \cdot (E \cdot Ez) \tag{3.116}$$

$$\dot{E}z = -k_9 \cdot E \cdot Ez + k_{10} \cdot (E \cdot Ez) + k_7 \cdot (E \cdot Ez) \tag{3.117}$$

$$\frac{d(E \cdot Ez)}{dt} = k_9 \cdot (E) \cdot (Ez) - k_{10} \cdot (E \cdot Ez) - k_7 \cdot (E \cdot Ez) \tag{3.118}$$

Then the set point of single-E controller in zero-order condition is

$$A_{set} = \frac{k_7 \cdot Ez_{tot}}{k_5} \tag{3.119}$$

Motif 2 dual-E controller with random order ternary complex mechanism

The rate equations for dual-E controller in Fig.3.25 are

$$\dot{A} = k_1 - k_2 \cdot A - k_4 \cdot A + \frac{k_3 \cdot k_8}{k_8 + E_1} \tag{3.120}$$

$$\dot{E}_1 = k_5 \cdot A - k_9 \cdot (E_1) \cdot (Ez) + k_{10} \cdot (E_1 \cdot Ez) - k_{15} \cdot (Ez \cdot E_2) \cdot (E_1) + k_{16} \cdot (E_1 \cdot Ez \cdot E_2) \tag{3.121}$$

$$\dot{E}_2 = k_6 - k_{11} \cdot (E_1 \cdot Ez) \cdot (E_2) + k_{12} \cdot (E_1 \cdot Ez \cdot E_2) - k_{13} \cdot (E_2) \cdot (Ez) + k_{14} \cdot (Ez \cdot E_2) \tag{3.122}$$

$$\dot{Ez} = -k_9 \cdot (E_1) \cdot (Ez) + k_{10} \cdot (E_1 \cdot Ez) - k_{13} \cdot (E_2) \cdot (Ez) + k_{14} \cdot (Ez \cdot E_2) + k_7 \cdot (E_1 \cdot Ez \cdot E_2) \tag{3.123}$$

$$\frac{d(E_1 \cdot Ez)}{dt} = k_9 \cdot (E_1) \cdot (Ez) - k_{10} \cdot (E_1 \cdot Ez) - k_{11} \cdot (E_1 \cdot Ez) \cdot (E_2) + k_{12} \cdot (E_1 \cdot Ez \cdot E_2) \tag{3.124}$$

$$\frac{d(E_1 \cdot Ez \cdot E_2)}{dt} = k_{11} \cdot (E_1 \cdot Ez) \cdot (E_2) + k_{15} \cdot (Ez \cdot E_2) \cdot (E_1) - (k_7 + k_{12} + k_{16}) \cdot (E_1 \cdot Ez \cdot E_2) \tag{3.125}$$

$$\frac{d(Ez \cdot E_2)}{dt} = k_{13} \cdot (E_2) \cdot (Ez) - k_{14} \cdot (Ez \cdot E_2) - k_{15} \cdot (Ez \cdot E_2) \cdot (E_1) + k_{16} \cdot (E_1 \cdot Ez \cdot E_2) \tag{3.126}$$

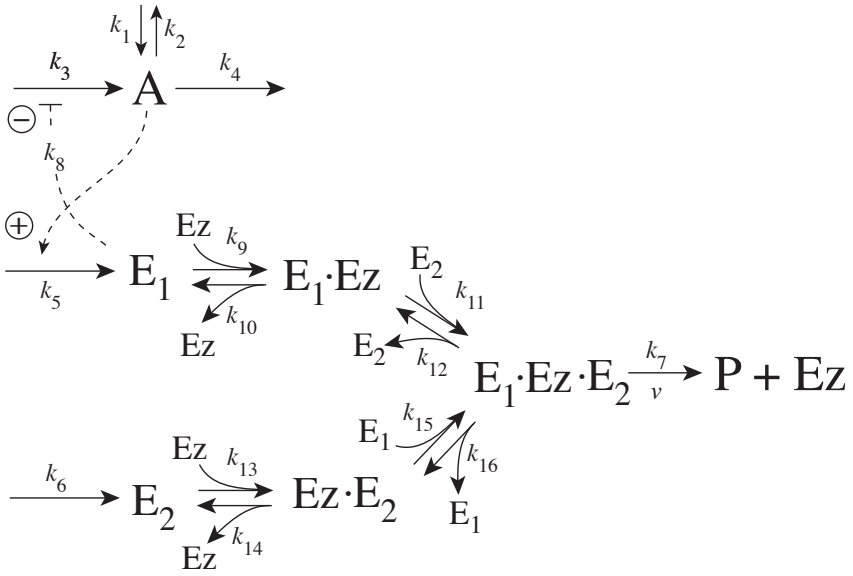

FIGURE 3.25: Motif 2 dual-E controller: removal of E_1 and E_2 by enzyme Ez using a ternary complex mechanism with random binding order.

Similar to motif 5-based controllers, motif 2 catalyzed antithetic dual-E controller can have two ways to calculate its set point when it has a zero-order condition. One is

$$A_{set} = \frac{k_6}{k_5} \tag{3.127}$$

The other is

$$A_{set} = \frac{k_7 \cdot Ez_{tot}}{k_5} \tag{3.128}$$

which is the same as for the set point of single-E controller.

Comparing the catalyzed motif 2 controllers: set point defence with step-wise perturbations

Fig.3.26 shows the performance of motif 2 dual-E and single-E controllers encountering the step-wise perturbations. For the upper left panel, it is easy to observe that dual-E controller can defend its set point no matter whether zero-order or non zero-order condition are applied. However, the single-E controller (Fig.3.26 the lower left panel) fails and shows an increasing off-set with increasing k_2 values. It is interesting to note that dual-E controller breaks down in perturbation 3. The reason for this is because an increasing k_2 leads to a saturation of Ez by E_2 such that E_1 cannot decrease to keep its set point (Fig.3.26 the upper right panel).

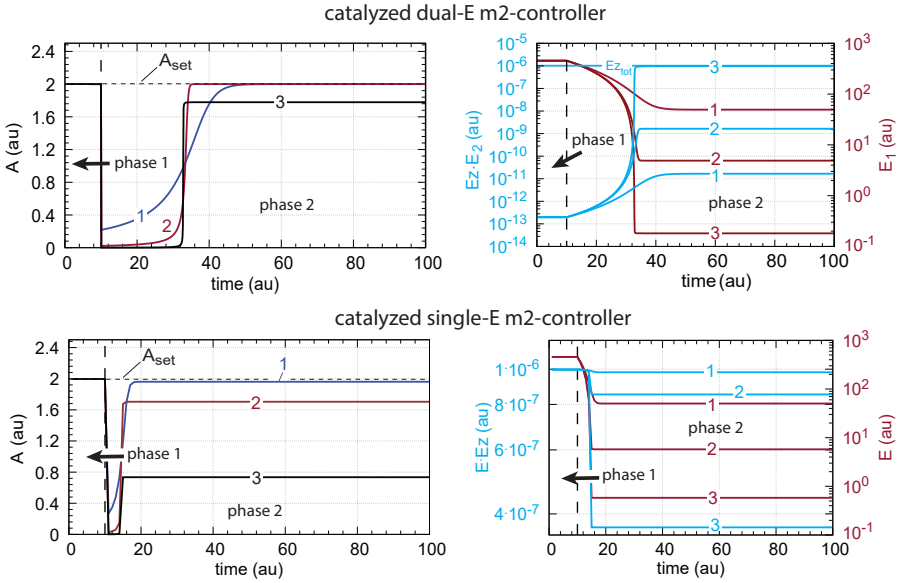

FIGURE 3.26: The comparison of motif 2 single-E and dual-E controllers to defend a set point. Upper left panel: Behavior of controlled variable A for dual-E controller. Phase 1: k_2=10.0; phase 2: 1, k_2=1×10^{+2}; 2, k_2=1×10^{+3}; 3, k_2=2×10^{+4}. Upper right panel: Behavior of manipulated variables E_1 and $Ez{\cdot}E_2$ for dual-E controller. Rate constants: k_1=0.0, k_3=1×10^{+5}, k_4=1.0, k_5=10.0, k_6=20.0, k_7=1×10^{+9}, k_8=0.1, k_9=1×10^{+8}, k_{10}=1×10^{+3}, k_{11}=1×10^{+8}, k_{12}=1×10^{+3}, k_{13}=1×10^{+8}, k_{14}=1×10^{+3}, k_{15}=1×10^{+8}, k_{16}=1×10^{+3}. Lower left panel: Behavior of controlled variable A for single-E controller. Same step-wise perturbation k_2 as in dual-E controller. Lower right panel: Behavior of manipulated variables E_1 and $Ez{\cdot}E_2$ for single-E controller. Rate constants are same as in dual-E controller except that k_5=50.0 and k_7=1×10^{+8}. Total enzyme concentration Ez_{tot}=1×10^{-6}.

Switching between dual-E and single-E control mode for motif 2 catalyzed antithetic controllers

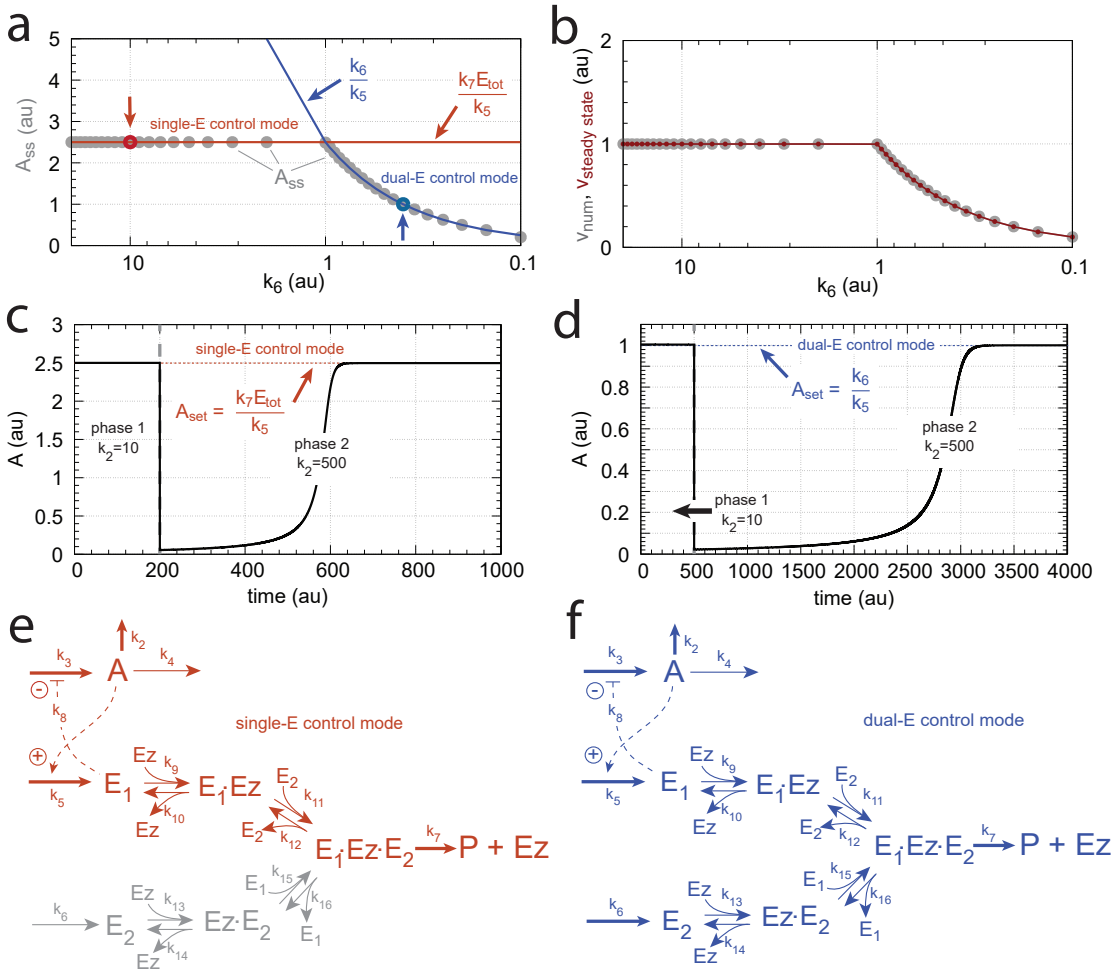

FIGURE 3.27: Switch between single-E and dual-E control mode in motif 2 catalyzed antithetic controller, with random order ternary complex mechanism in the removal of E_1 and E_2. (**a**) A_{ss} as a function of k_6. The A value for single-E and dual-E control mode are showed in red line and blue line respectively. The gray solid points mean the numerically calculated steady state values. The outlined red and blue circles show the k_6 values (10.0 and 0.4) used in panels **c** and **d**. (**b**) Steady state values of v calculated by King-Altman method (red line) and numerical velocities (gray points). (**c**) and (**d**) Single-E and dual-E control mode with k_6 equaling 10.0 and 0.4 respectively. Rate constants: k_2 applies step-wise from 10.0 to 500.0, k_1=0, k_3=1×10^{+5}, k_4=1.0, k_5=0.4, k_7=1×10^{+6}, k_8=0.1, k_9=1×10^{+8}, k_{10}=1×10^{+3}, k_{11}=1×10^{+8}, k_{12}=1×10^{+3}, k_{13}=1×10^{+8}, k_{14}=1×10^{+3}, k_{15}=1×10^{+8}, k_{16}=1×10^{+3}. (**e**) The part of the network outlined in red is active during single-E control mode. (**f**) The entire network is active during dual-E control mode outlined in blue.

A switching between dual-E and single-E control mode in motif 2-based controllers can also be observed in Fig.3.27. As the equations derivation before, the set point of dual-E

controller depending on the relative values of k_6 and $k_7{\cdot}Ez_{tot}$, we have the equation

$$A_{set} = \frac{k_6}{k_5} = \frac{k_7{\cdot}Ez_{tot}}{k_5} \tag{3.129}$$

As the results show, when

$$\frac{k_6}{k_5} \geq \frac{k_7{\cdot}Ez_{tot}}{k_5} \tag{3.130}$$

the value of $k_7{\cdot}Ez_{tot}/k_5$ is lower than $\frac{k6}{k5}$ and only part of dual-E controller is functioning properly, i.e., the dual-E controller works in single-E control mode (Fig.3.27 **c** and **e**). When

$$\frac{k_6}{k_5} < \frac{k_7{\cdot}Ez_{tot}}{k_5} \tag{3.131}$$

dual-E controller follows the behavior of general dual-E control mode and all manipulated variables participate in the regulation (Fig.3.27 **d** and **f**). The same behavior is found for non zero-order condition. dual-E controller follows the behavior of general dual-E control mode and all manipulated variables participate in the regulation (Fig.3.27 **d** and **f**). The same behavior is found for non zero-order condition.

Conclusion and Perspectives

Conclusion of the comparison between motif 5-based and motif 2-based controllers

As the results show, we have the following conclusions when comparing motif 5-based and motif 2-based controllers:

1. Both uncatalyzed antithetic controller and zero-order integral controller for motif 5 and motif 2 can keep their homeostatic function for step-wise perturbations.

2. While as for the linear increased perturbation, motif 2-based controllers show a better ability than the motif 5-based controllers to defend set points with increasing k_7 values and leading to an increasing accuracy.

3. A higher aggressiveness will shorten the reaction response time.

4. As considering an explicitly enzyme catalyzed degradation, the antithetic dual-E controllers show a more robust system than the single-E controllers, both for motif 5-based and motif 2-based controller. The dual-E controllers can maintain homeostasis even at non zero-order condition, while single-E controllers can not.

5. Particularly, different two-substrate enzyme mechanisms, including ternary complex compulsory order, ternary complex random order and substitution (ping-pong) mechanism, are studied within motif 5-based controllers and show no significant difference.

6. It is noteworthy that there is a switching in the dual-E controller between dual-E and single-E control mode. The switching depends on the relative values of k_6 and $k_7 \cdot Ez_{tot}$ and applies for both motif 5-based and motif 2-based controllers. When k_6 is lower than $k_7 \cdot Ez_{tot}$, the dual-E controller switches to a single-E control mode. When, k_6 is larger than $k_7 \cdot Ez_{tot}$, the dual-E controllers work in dual-E control mode.

Consider that motif 5 and motif 2 are the in-loop controllers (Fig.1.3) and they show a switch. A further investigation should be done with the out-loop controller, such as motif 4 and motif 7, which is expected, that they may break down directly, or there is no switch situation at all.

7. A difference between motif 5-based and motif 2-based controllers is the behaviors of A with an increasing perturbations under a non zero-order condition, k_1 for motif 5-based controllers and k_2 for motif 2-based controllers, respectively. An increasing perturbation will decrease the off-set from A_{ss} to A_{set} for motif 5-based controllers, while an increasing off-set for motif 2-based controllers is observed.

Perspectives

In this thesis, we have dealt with the components, such as A, Ez, E_1 and E_2, but we do not assign any specific name. From a physiological view, they could represent different components, respectively, and there are many possibilities. For example, the manipulated variable and controlled variable can represent the reaction constituent, the energy substance (ATP and ADP), and the enzyme (NAD^+ [16]) etc.

For example, Fig.4.1 can represent a protein kinase reaction corresponding with motif 2 catalyzed antithetic dual-E controller with random order ternary complex mechanism (Fig.3.25). E_1, an inhibitor of the regulated compound A, is phosphorylated by the kinase (Ez) requiring the existence of ATP (E_2) to produce product P. The vast majority of protein kinases follow the random order ternary complex mechanisms and few of them follow ping-pong mechanisms [17].

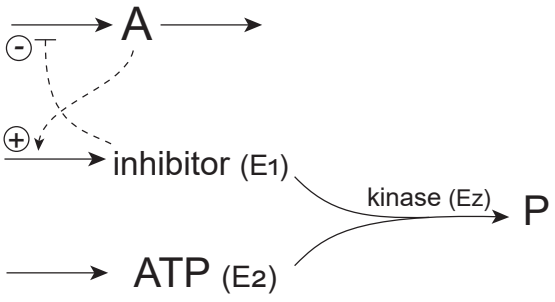

FIGURE 4.1: A protein kinase reaction, corresponding with Fig.3.25, follows random order ternary complex mechanism. E_1: inhibitor; E_2: ATP; Ez: kinase, respectively.

An opinion from N.Mrosovsky proposed in *Rheostasis* [18], is that the set point in homeostatic systems may change and could exhibit the new set points. We have some results (Fig.3.20 **a** and Fig.3.27 **a**) proving this kind of change, which reminds us of a fever, i.e., a temperature change to a higher set point during illness.

In our research, we assume the synthesis of final product P is an irreversible reaction, which is corresponding the opinion from Lotka. Lotka found that "homeostasis can be explained by *Le Chatelier's principle*" is incorrect [19]. Take Fig.3.25 as an example. If it is reversible in k_7, product P can not go into a steady state but increasing continuously because of the increasing ternary complex $E_1 \cdot Ez \cdot E_2$ according to the *Equilibrium Law*. Practically, all life reactions are irreversible, which is in line with reality.

Appendix

Matlab programs. A zip-file with Matlab programs showing the results from Fig.3.17 is attached to this thesis.

Bibliography

[1] Corentin Briat, Ankit Gupta, and Mustafa Khammash. Antithetic integral feedback ensures robust perfect adaptation in noisy biomolecular networks. *Cell Systems*, 2 (1):15–26, 2016.

[2] Walter B Cannon. Organization for physiological homeostasis. *Physiological Reviews*, 9(3):399–431, 1929.

[3] Steven J Cooper. From Claude Bernard to Walter Cannon. Emergence of the concept of homeostasis. *Appetite*, 51(3):419–427, 2008.

[4] Leroy Lester Langley. *Homeostasis: Origins of The Concept*. Dowden Hutchinson and Ross, 1973.

[5] Gunhild Fjeld, Kristian Thorsen, Tormod Drengstig, and Peter Ruoff. Performance of homeostatic controller motifs dealing with perturbations of rapid growth and depletion. *The Journal of Physical Chemistry B*, 121(25):6097–6107, 2017.

[6] J Wilkie, M Johnson, and K Reza. *Control Engineering. An Introductory Course*. Palgrave, 2002.

[7] T Drengstig, IW Jolma, XY Ni, K Thorsen, XM Xu, and P Ruoff. A basic set of homeostatic controller motifs. *Biophysical Journal*, 103(9):2000–2010, 2012.

[8] Jordan Ang, Sangram Bagh, Brian P Ingalls, and David R McMillen. Considerations for using integral feedback control to construct a perfectly adapting synthetic gene network. *Journal of Theoretical Biology*, 266(4):723–738, 2010.

[9] Peter Ruoff, Oleg Agafonov, Daniel M Tveit, Kristian Thorsen, and Tormod Drengstig. Homeostatic controllers compensating for growth and perturbations. *PloS One*, 14(8), 2019.

[10] Stephanie K Aoki, Gabriele Lillacci, Ankit Gupta, Armin Baumschlager, David Schweingruber, and Mustafa Khammash. A universal biomolecular integral feedback controller for robust perfect adaptation. *Nature*, 570(7762):533–537, 2019.

[11] James E Ferrell Jr. Perfect and near-perfect adaptation in cell signaling. *Cell Systems*, 2(2):62–67, 2016.

[12] Irwin H Segel. *Enzyme kinetics: Behavior and Analysis of Rapid Equilibrium and Steady State Enzyme Systems.* John Wiley & Sons, 1975.

[13] W W Cleland. The kinetics of enzyme-catalyzed reactions with two or more substrates or products: I. nomenclature and rate equations. *Biochimica et Biophysica Acta (BBA)-Specialized Section on Enzymological Subjects*, 67:104–137, 1963.

[14] K. Radhakrishnan and A.C. Hindmarsh. *Description and Use of LSODE, the Livermore Solver for Ordinary Differential Equations. NASA Reference Publication 1327, Lawrence Livermore National Laboratory Report UCRL-ID-113855.* National Aeronautics and Space Administration, Lewis Research Center, Cleveland, OH 44135-3191, 1993.

[15] John W Moore and Ralph G Pearson. *Kinetics and Mechanism.* John Wiley & Sons, 1981.

[16] Richard A Billington, Santina Bruzzone, Antonio De Flora, Armando A Genazzani, Friedrich Koch-Nolte, Mathias Ziegler, and Elena Zocchi. Emerging functions of extracellular pyridine nucleotides. In *Molecular Medicine*, volume 12, pages 324–327. BioMed Central, 2006.

[17] Zhihong Wang and Philip A Cole. Catalytic mechanisms and regulation of protein kinases. In *Methods in Enzymology*, volume 548, pages 1–21. Elsevier, 2014.

[18] Nicholas Mrosovsky. *Rheostasis: The Physiology of Change.* Oxford University Press, 1990.

[19] Alfred J Lotka. *Elements of Physical Biology.* Williams & Wilkins Company, 1925.